



Contents lists available at ScienceDirect



Applied Clay Science

journal homepage: www.elsevier.com/locate/clay

Research paper

Illitization of Late Devonian-Early Carboniferous K-bentonites from Western Pontides, NW Turkey: Implications for their origin and age

Ömer Bozkaya ^{a,*}, Asuman Günal-Türkmenoğlu ^b, M. Cemal Göncüoğlu ^b, Özge Ünlüce ^b, İsmail Ömer Yilmaz ^b, Paul A. Schroeder ^c

^a Department of Geological Engineering, Pamukkale University, Denizli, Turkey

^b Department of Geological Engineering, Middle East Technical University, Ankara, Turkey

^c Department of Geology, University of Georgia, Athens, GA, USA

ARTICLE INFO

Article history:

Received 19 April 2016

Received in revised form 13 August 2016

Accepted 19 August 2016

Available online xxxx

Keywords:

K-bentonite

Illitization

Diagenesis

Mineralogy

Geochemistry

NW Turkey

ABSTRACT

K-bentonite (tephra) layers are exposed as thin beds within Late Devonian-Early Carboniferous carbonates of the Yılanlı formation at four different locations in northwestern, Turkey. Clays separated from K-bentonites in the Gavurpinarı, Yılanlı Burnu (Bartın) and Çimşir Çukurları (Şapça) quarries and the Güdüllü-Gökgöl highway tunnel section near Zonguldak were analyzed by X-ray diffraction, optical, scanning and high-resolution transmission electron microscopy and inductively coupled plasma-mass spectrometry. The clay mineralogy is dominated by illite and mixed-layer illite-smectite (I-Sm) along with subordinate amounts of kaolinite, dolomite, calcite, quartz, feldspar, and gypsum. Morphologically, platy shaped illite is the major clay mineral in the Gavurpinarı and Yılanlı Burnu sites, while sponge-like to platy shaped mixed-layer illite-smectites occur in the Şapça Çimşir Çukurları and Gökgöl sites. Illite Kübler index (KI, Δ^20) and polytype data indicate high-grade diagenesis for illite-bearing site, and low-grade diagenesis for I-Sm-bearing sites. Lattice d_{006} values (\AA) of illite and I-Sm reflect a dioctahedral composition, with relatively larger d_{006} values in the Yılanlı Burnu site, which is related to Mg incorporation into the octahedral layer from dolomitic limestone host-rocks. Illites have relatively lower tetrahedral Al substitution and higher octahedral Fe and Mg substitutions compared to those of I-Sm. Illites with at phengitic composition occur in the Gavurpinarı and Yılanlı Burnu sites, whereas muscovitic composition for Şapça Çimşir Çukurları site. Chondrite-normalized rare earth element patterns for the Gavurpinarı and Yılanlı Burnu sites exhibit similar trends, with relatively higher values when compared to trends for the Şapça Çimşir Çukurları sites. Oxygen ($\delta^{18}\text{O}$) isotope values of illites and I-Sm range from 17.7 to 21.9‰ (V-SMOW), whereas hydrogen (δD) isotope values range widely from -10.1 to -69.9 ‰ (V-SMOW). The depleted values of $\delta^{18}\text{O}$ values for the Gavurpinarı site imply geologically sudden crystallization under higher temperature conditions. K/Ar ages of different size illite fractions indicate the presence of older detrital illites ($2 \mu\text{m}$) together with younger diagenetic fractions ($0.5 \mu\text{m}$) that correspond with an increase of $2M_1$ polytype in the coarser fraction. Illitization ages of K-bentonites in the Bartın area indicate an Early Permian event corresponding to the Variscan orogeny, whereas the illitization of K-bentonites in the Zonguldak area is Early Jurassic in age, related to the Cimmerian deformation in the region.

© 2016 Published by Elsevier B.V.

1. Introduction

K-bentonites yield a special case for illite formation in sedimentary rocks under diagenetic conditions because they act as relatively closed systems. The products of explosive eruptions in the form of wind-born volcanic ash (tephra) deposited after being transported for long distances, which are then altered to bentonites (smectite-rich volcanicogenic clay rocks) during low-grade diagenesis. During high-

grade diagenesis ($>100^\circ\text{C}$), these bentonites are transformed into K-bentonites by K-fixation (Huff and Türkmenoğlu, 1981). Progressive illitization also occurs by low-grade metamorphism (in the range of 40° to 100°C), which finally results in the formation of meta-bentonites (Fortey et al., 1996). During diagenesis and/or very low-grade metamorphism smectite transforms to mixed-layer illite-smectite (I-Sm) and then illite in K-bentonites (Weaver, 1953; Nadeau et al., 1985; Merriman and Roberts, 1990). Old bentonite occurrences often contain illite-rich I-Sm (Elliot and Aronson, 1987; Histon et al., 2007) and in some cases, very old ones can have almost pure illites (Moe et al., 1996).

Illitization has been widely used as a tracer for reconstructing the evolution of sedimentary basins and hydrothermal

* Corresponding author.

E-mail address: obozkaya@pau.edu.tr (Ö. Bozkaya).

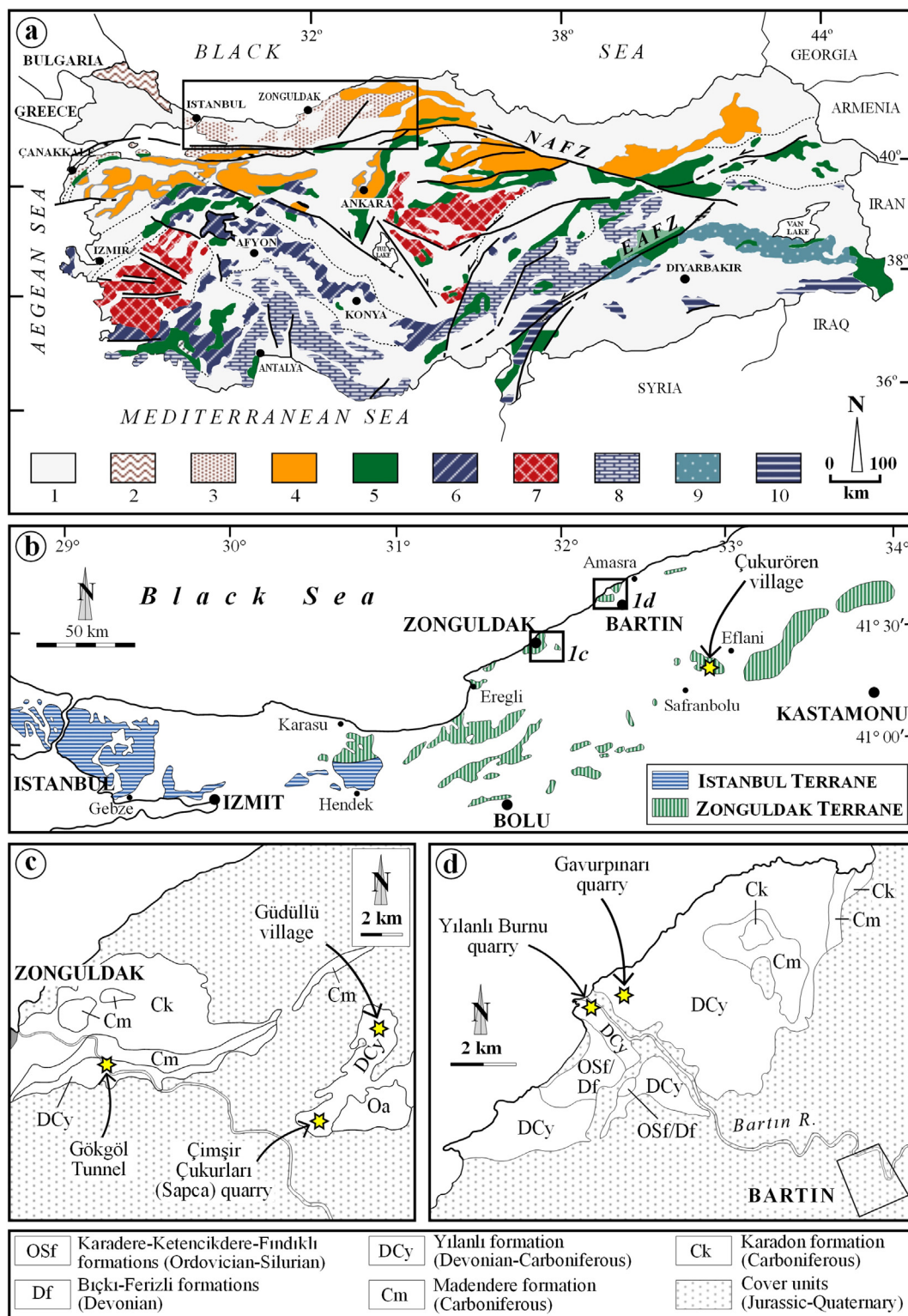


Fig. 1. (a) Alpine tectonic units of Turkey (Göncüoğlu et al., 1997) and location of the İstanbul and Zonguldak terranes (NAFZ: North Anatolian Fault Zone, EAFZ: East Anatolian Fault Zone. Symbols: 1: Tertiary cover; 2: Istranca Terrane, 3: İstanbul-Zonguldak Terrane, 4: Sakarya Composite Terrane, 5: ophiolites and ophiolitic mélange of Neotethyan Suture Belts, 6: Kütahyal-Bolkardağ Belt (Anatolides), 7: Menderes and Central Anatolian Crystalline Complexes (Anatolides), 8: Taurides, 9: Bitlis-Pötürge Metamorphics (SE Anatolian Autochthon), 10: SE Anatolian Autochthon), (b) The distribution of the Paleozoic outcrops in the İstanbul and Zonguldak terranes (modified from Bozkaya et al., 2012), (c-d) Geological maps of the study areas and geographic settings of sampling locations (modified from Akbaş et al., 2002).

environments. It is generally considered to proceed as a continuous process mainly driven by temperature increase and interaction with interstitial fluids during progressive burial (Schroeder, 1992). Stable isotope and K/Ar, Ar/Ar data of authigenic illite and

I-Sm crystals provide important data for evaluation of the duration and mechanism of burial-induced illitization (e.g., Clauer et al., 1997; Środoń et al., 2002, 2006; Honty et al., 2004; Clauer, 2006).

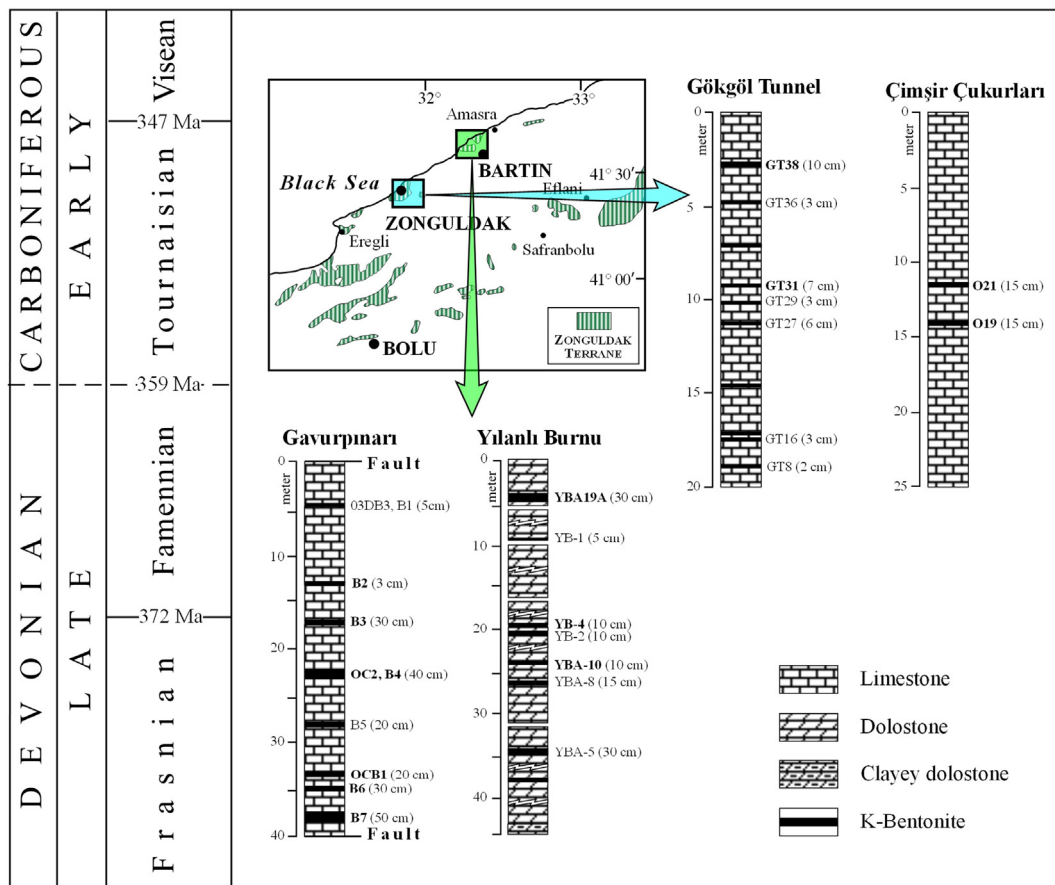


Fig. 2. The distribution of the Devonian-Carboniferous sequences of the Yılanlı Formation in NW Anatolia with the position of the K-bentonite layers.

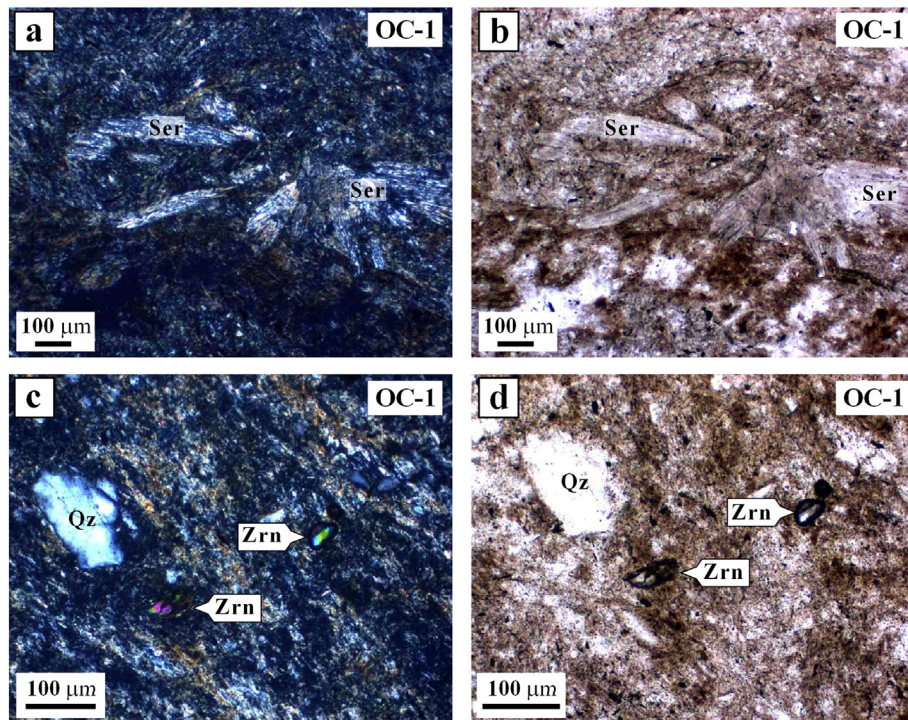


Fig. 3. Photomicrographs of K-bentonite samples from Gavurpinari quarry (from Göncüoğlu et al., 2016). (a-b) Pyroclastic (vitroclastic) textured K-bentonite sample from Gavurpinari quarry with sericitized volcanic matrix and shards of glass (or pumices) of (a)-crossed nicols-cn, b-plain polarized light-ppl). (c-d) Sub- to anhedral and slightly rounded subhedral zircon crystals within the sericitized volcanic matrix of K-bentonite sample from Gavurpinari quarry (c-cn, b-ppl).

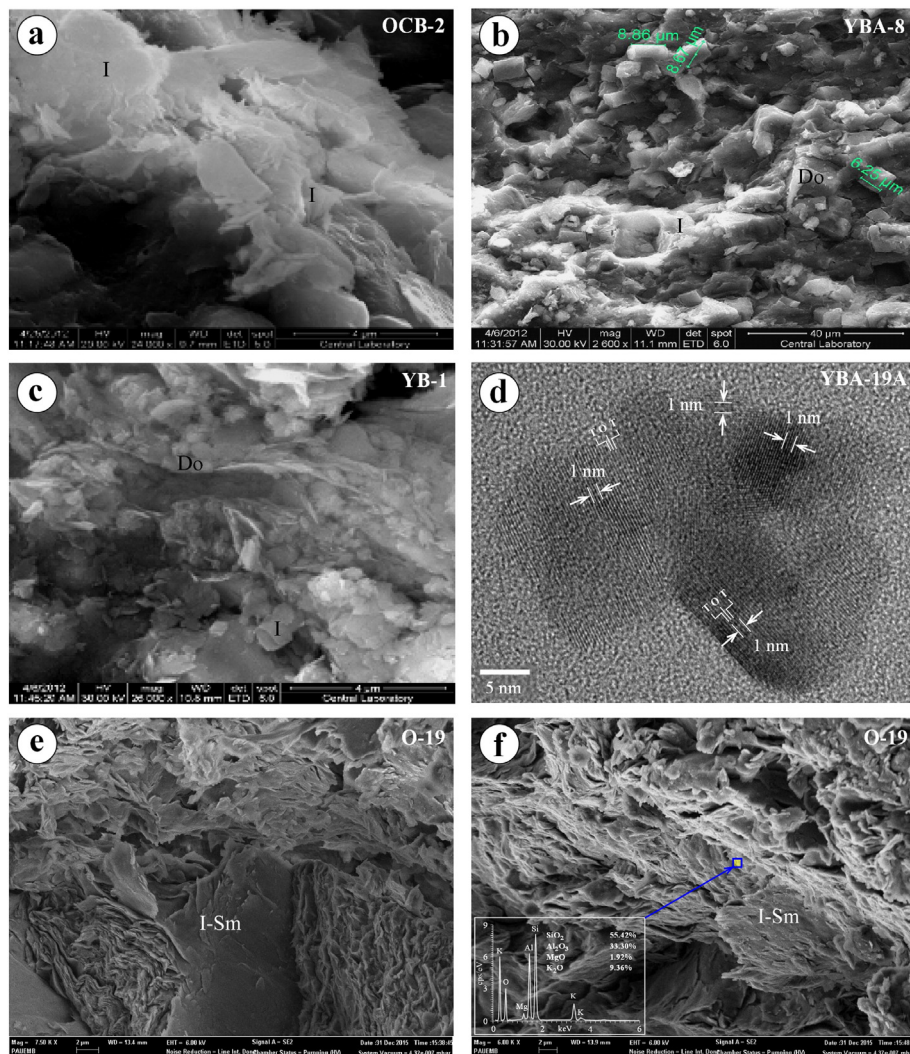


Fig. 4. (a) SEM photomicrographs display platy and juxtaposed structure of illites in sample from Gavurpinarı quarry, (b–c) Platly and fibrous illites and associated dolomite crystals in samples from Yılanlı Burnu quarry, (d) HR-TEM microphotograph shows regular stacking sequence of illites (10 \AA) in sample YBA-19A from Yılanlı Burnu quarry (from Günal-Türkmenoğlu et al., 2015), (e–f) Sponge-like to platy R3 I-Sm and its chemical composition in sample from Çimşir Çukurları quarry.

Although extensive studies have been published on worldwide K-bentonites of volcanic origin, their occurrence in Turkey has only been recently recognized (Türkmenoğlu, 2001; Türkmenoğlu et al., 2009; Günal-Türkmenoğlu et al., 2015; Göncüoğlu et al., 2016). K-bentonite layers were found alternating with platform type limestone and dolomitic limestones of the Middle Devonian-Lower Carboniferous age Yılanlı Formation in the Zonguldak and Bartın areas at the western Black Sea region (Fig. 1). They occur at four different locations, including quarries in the Gavurpinarı, Yılanlı Burnu (Bartın), Çimşir Çukurları (Şapça) and in the Güdüllü-Gökgöl highway tunnel section near Zonguldak (Fig. 1). These recent K-bentonite studies in NW Turkey describe their geological distribution, stratigraphic position, and basic mineralogical properties. These K-bentonites have event-stratigraphic significance for regional correlation to interpret the paleogeographic, tectonic, and magmatic setting of source volcanoes (Günal-Türkmenoğlu et al., 2015; Göncüoğlu et al., 2016).

The present study focuses on understanding the origin and age of illitization of tephras in the Bartın and Zonguldak areas to provide additional context for the geological history of the region. The basis for this work is detailed mineralogical (crystal-chemical) and geochemical

data (i.e., major, trace, rare earth element, stable oxygen and hydrogen isotope, and K-Ar age dating).

2. Geological setting

The study area is located at the Bartın-Zonguldak area, in northwest Anatolia (Fig. 1a) where K-bentonite beds have recently been recognized. They are intercalated within limestone and dolomitic limestone successions of the Yılanlı formation, which are Middle Devonian-Early Carboniferous in age. The northwestern Black Sea region consists of an accretionary terrane assemblage (Göncüoğlu and Kozur, 1998, 1999; Göncüoğlu and Kozlu, 2000; Yanev et al., 2006) comprised by two different Gondwanan microplates (e.g. Göncüoğlu et al., 1997) that include the İstanbul terrane (IT) in the West and the Zonguldak terrane (ZT) in the East (Fig. 1b). The main differences between ZT and IT are their divergent stratigraphy and the presence of a Caledonian thermal event in the ZT (Bozkaya et al., 2012).

K-bentonites in this study are restricted to the ZT and have not been reported from any other parts of the İstanbul-Zonguldak terrane or their equivalents in surrounding Paleozoic terranes such as Moesia, Balkans

Table 1

Bulk and clay fraction mineralogic composition of K-bentonites.

Örnek no	XRD - whole rock						XRD - clay fraction		
	Calcite	Dolomite	Quartz	Feldspar	Clay	Other minerals	Illite	Kaolinite	I-Sm
<i>Yılanlı Burnu Quarry</i>									
YBA-2	++++	±	±	+	Ant	+++++	±		
YBA-5	+++	±	±	++	Ant	++++	±		
YBA-8	++	±	±	+++	Ant	++++			
YBA-10	++	±	±	+++	Ant	++++			
YBA-19A	++	±	±	+++	Py, Ant	++++			
YB-1	++++	±	±	+	Gt/Lm	++++	±		
YB-2	+	±	±	++++	Ant	++++			
YB-4	++	±	±	+++	Ant	++++			
<i>Gavurpinarı Quarry</i>									
KRD-B-1	+		±	++++	Ant	++++			
KRD-B-2	+		+	++	Gt(2), Ant	++++			
KRD-B-3	+		+	++	Gt(1), Ant	++++			
KRD-B-4			+	+++	Gp(3), Ant	++++			
KRD-B-5	±		+	+++	Gt/Lm(13), Ant	++++			
KRD-B-6		++	+	++	Gp(2), Ant	++++			
KRD-B-7	+	±	+	++	Gp(6)	++++			
OCB-1G	+		+	++	Gp(3), Ant	++++			
OCB-1S			+	+++	Ant, Gt/Lm	++++			
OCB-2 A	++	±	+	++	Gp(1), Ant	++++			
OCB-2B	++	±	+	++	Gt, Ant	++++			
OC1-B3			+++	++	Gp(3), Alu	+	++		++
OCC-2	++++		±	+	Ant	++++			
<i>Çukurören Village</i>									
Ö-5	++	+		++	Ant	+++	+		
Ö-12	++	+		++	Ant	++++	±		
Ö-17 A	±		+	+++	Ant	+++			+
<i>Sapçı Çimşir Çukurları Quarry</i>									
Ö-19B				+++++	Ant(7), Py(3)				++++
Ö-21	+			+++	Ant(9), Py(5), Jrs				++++
<i>Gökgöl Tunnel</i>									
GT-3		+		++++	Ant, Gt				++++
GT-16	±		+	+++	Ant, Gt				++++
GT-27		±	+	+++	Gp(4), Ant, Gt				++++
GT-29	+		+	++	Gp(1), Ant, Gt				++++
GT-31			±	++++	Gp(1), Ant, Gt				++++
GT-38				++++	Ant, Gt, Jrs				++++

Ant: anatase, Py: pyrite, Gt: goethite, Lm: limonite, Gp: gypsum, Jrs: jarosite, +: 20%, ±: Rare.

or Caucasus. Tephra-layers are thought to have formed in relation to arc-volcanism, generated by the closure of the Variscan Rheic Ocean (Nzegge et al., 2006; Okay et al., 2010; Bozkaya et al., 2012; Göncüoğlu et al., 2016).

The basement Cadomian crystalline rocks in the ZT are unconformably overlain by Lower Ordovician units (Göncüoğlu et al., 2014), comprising siltstones, mudstones (Bakacak Formation) and conglomerates and sandstones (Kurtköy and Aydos Formations). The Upper Ordovician to Middle Silurian succession is represented by the Karadere, Ketencikdere, and Findıklı Formations containing graptolitic black and grey shale, sand- and, siltstones (Sachanski et al., 2010) with limestone interlayers (Dean et al., 1997). The Findıklı Formation is unconformably overlain by the Middle Devonian Bıçkı and Ferizli formations consisting of sandstones-mudstones and shales-siltstones, respectively. The Late Middle Devonian - Late Early Carboniferous (Sepukovian) Yılanlı Formation hosts the K-bentonite layers. It includes shallow-marine dolomites and limestones succeeded by the Middle Devonian shales-siltstones (Ferizli Formation, (Aydin et al., 1987; Derman, 1997; Yalçın and Yılmaz, 2010; Bozkaya et al., 2012). The Yılanlı Formation is composed of grey, dark grey, black, medium to thick-bedded limestones, dolomitic limestones and dolomites alternating with thin-bedded, black, calcareous shales. The approximate thickness of the Yılanlı Formation is 800 m. Gedik et al. (2005) report that the Ferizli and Madendere Formations have transitional boundaries to the Yılanlı Formation. Foraminifera (Dil, 1976) indicate an Eifelian-Visean age (Middle Devonian-

Early Carboniferous) for the Yılanlı Formation. The deposition of the Yılanlı Formation continued from the Middle Devonian to Early Carboniferous in a marine carbonate platform/shelf (Yalçın and Yılmaz, 2010). The formation is overlain by a >500 m thick sequence of alternating limestones and shales (Madendere and Karadon formations), followed by flood-plain deposits with numerous coal-stems of Westphalian age (Kerey, 1984). The oldest cover of the Variscan units of the Zonguldak Terrane are the Upper Permian (Tatarian) lagoonal sediments (Göncüoğlu et al., 2011) followed by the Upper Triassic continental red beds of the Çakraz Formation (Alişan and Derman, 1995).

The studied K-bentonite beds occur in the upper part of the Yılanlı Formation. The geological details of the measured sections of the Bartın (Gavurpinarı and Yılanlı Burnu sections) and Zonguldak (Şapça Çimşir çukurları and Gökgöl) areas (Fig. 1c, d) were given in Günal-Türkmenoğlu et al. (2015) and Göncüoğlu et al. (2016), respectively. The log of the Yılanlı Formation is shown in Fig. 2 for regional correlation. The K-bentonite layers in the Gavurpinarı and Yılanlı Burnu quarries are located stratigraphically in lower levels with respect to those in the Çimşir Çukurları quarry and the Gökgöl tunnel sections based on fossil data (Göncüoğlu et al., 2016). The marly limestones below the bentonitic beds include a few mm thick bands, very rich in ostracods. The K-bentonite bearing successions from the Gavurpinarı Quarry near Bartın are rich in calcareous microfossils indicating a late Frasnian age (Göncüoğlu et al., 2016).

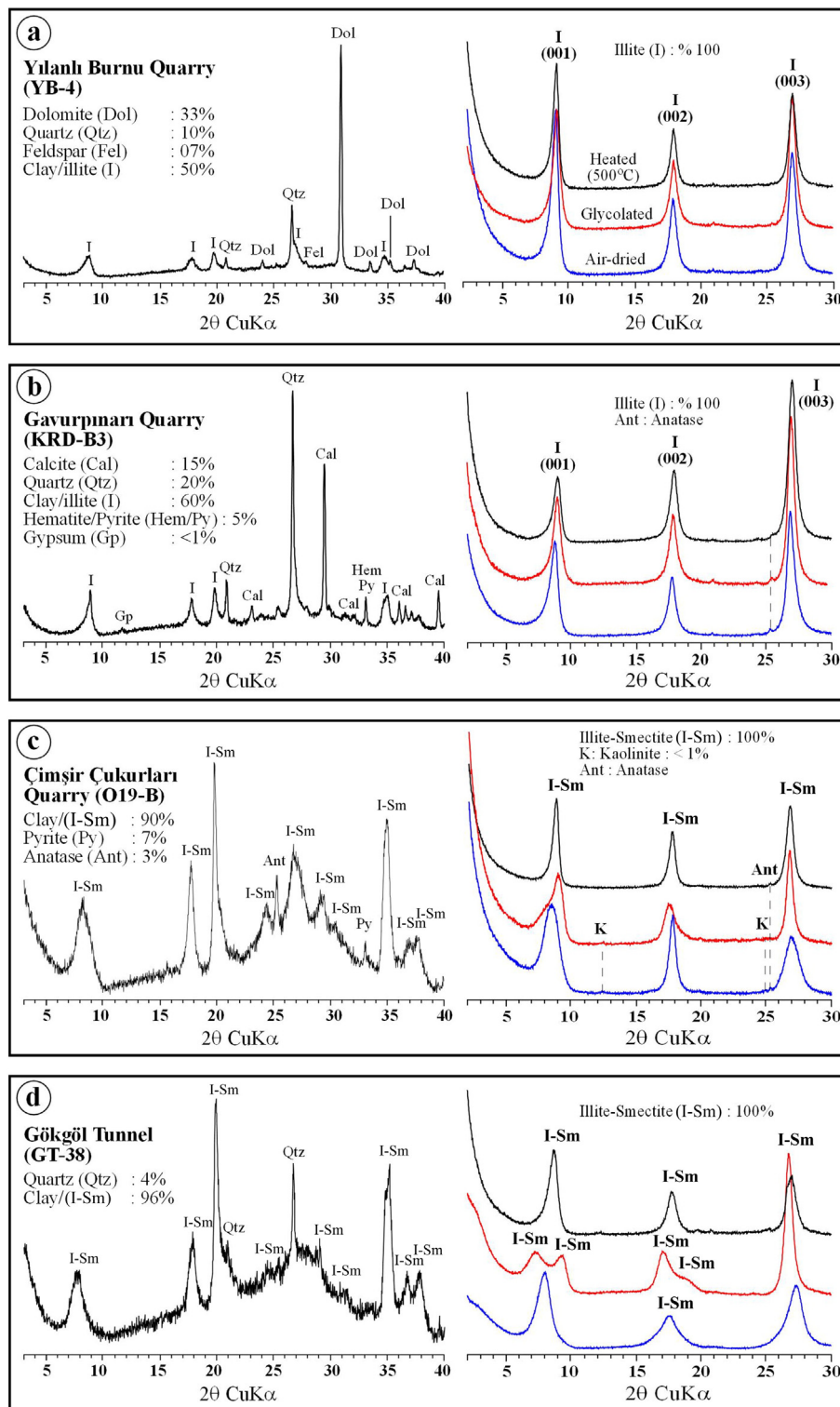


Fig. 5. XRD patterns of bulk and clay fractions of the representative K-bentonite samples from different areas.

3. Material and methods

A total of thirty-two pure and nearly pure illite and I-Sm-bearing samples were investigated by mineralogical methods and sixteen samples by chemical methods. Scanning and high-resolution transmission electron microscopes (SEM and HR-TEM) and X-ray powder diffractometer (XRD) in the Central Laboratory of the Middle

East Technical University (Ankara) and Pamukkale University (Denizli) were used for determining mineralogical properties. Major and trace element analysis were performed at the University of Georgia (Athens, Georgia, USA) and ACME Analytical Laboratories Ltd. (Vancouver, Canada). Oxygen and hydrogen analysis were performed on a Finnigan MAT 252 Mass Spectrometer at the University of Georgia.

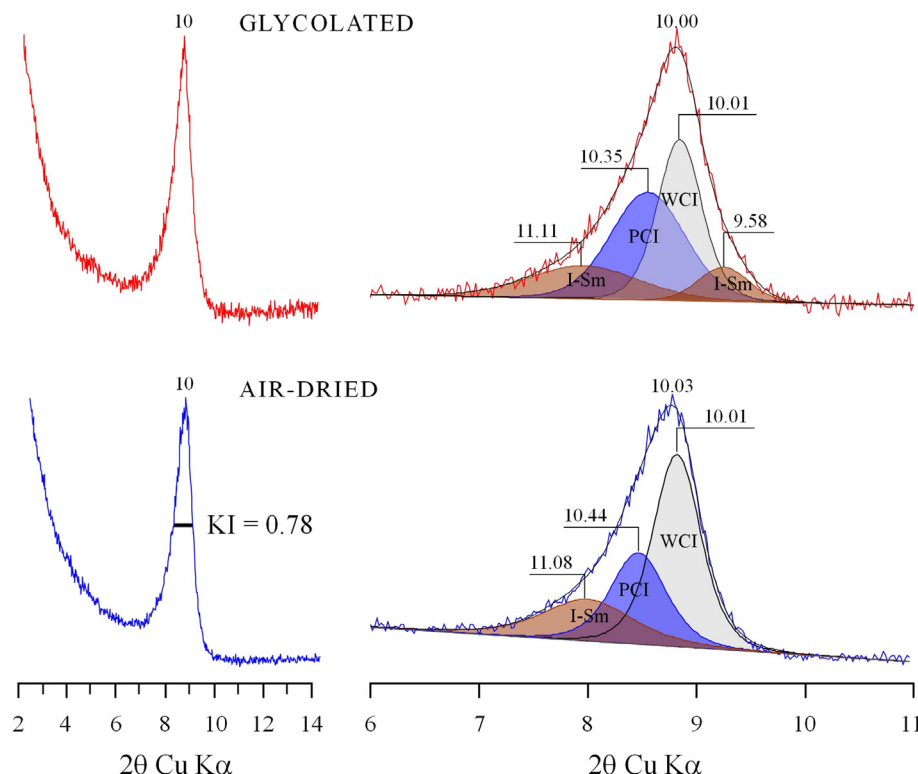


Fig. 6. Decomposition of illite peak showing well crystallized illites (WCI), poorly crystallized illite (PCI) and I-Sm phases in K-bentonite from the Yilanli Burnu quarry.

Bulk and clay mineralogy, and crystal-chemical data of illites were studied by XRD using a Rigaku Miniflex II diffractometer with CuK α radiation and a graphite monochromator. The X-ray tube was operated at 35 kV and 15 mA at a scanning speed of 2° 20/min. A slower rate of 1° 20/min was used for illite crystal-chemical characteristics (e.g., illite crystallinity; Kisch, 1991). Clay fractions (<2 μ m equivalent spherical diameter) were separated by dispersing the bulk sample in distilled water after acid-treatments to eliminate carbonate minerals, followed by sedimentation and centrifugation. Oriented mounts were obtained by thin-smeared clay paste on glass slides. Similar procedures were used to fractionate the clay fractions into finer grain sizes (1–2 μ m, 0.5–1 μ m, 0.25–0.5 μ m, <0.25 μ m). XRD patterns were obtained after the treatments of air-dried, ethylene glycolated, and heated at 500 °C states. For eliminating carbonate minerals, dilute acetic acid (10%) was preferred over hydrochloric acid because it less likely to affect clay crystallinity and/or structures. The diluted hydrochloric acid (5%) was used to eliminate carbonates in dolomite-bearing samples. Determinations of clay minerals from XRD patterns were based on the data of Hoffman and Hower (1979) and Moore and Reynolds (1997). Illite “crystallinity” (Kübler Index-KI; Kübler, 1968; Guggenheim et al., 2002) was determined by measuring the full width at half maximum (FWHM) at the first basal illite reflection near 10 Å in air-dried <2 μ m fractions of the K-bentonite samples. Crystallinity Index Standards (CIS, Warr and Rice, 1994) were used in the calibration of FWHM values to KI with the linear equation of $KI_{CIS} = 1.18 \times FWHM_{METU} - 0.015$, $r^2 = 0.999$. KI_{CIS} values re-calibrated with equation of Warr and Ferreiro-Mählmann (2015) to convert the original (Basel KI scale) upper and lower boundary limits of anchizone, 0.25°20 and 0.42°20.

Narrowing of the peak width suggests an increase in crystallinity due to larger scattering domains of illite resulting from collapse of interlayers and conversion of smectite to illite under increasing temperature and pressure conditions. Three main zones: low- and high-grade diagenetic zone (>1.00); anchizone (0.42–0.25); and epizone (<0.25) were distinguished for KI values (e.g., Frey, 1987; Merriman and Frey, 1999; Ferreiro Mählmann et al., 2012).

The intensity ratio [$Ir = I(I001) / I(I003)_{air-dried}/I(I001) / I(I003)_{ethylene-glycolated}$] data were realized for relative abundances of expandable (smectite) layers (Šrodoň, 1984). The contents of swelling smectite layers (smectite) in illites and ordering type (Reichweite = R, Jagodzinski, 1949; Reynolds, 1980) of I-Sm were determined following the XRD methods of Moore and Reynolds (1997). NEWMOD (Reynolds, 1985) and WINFIT (Krumm, 1996) programs were also applied for precise interpretation of mixed-layer clay minerals. Mean XRD scattering domain sizes and contents of swelling (smectitic) layers in illites were estimated using the NEWMOD-based graphs (KI vs. Ir) calculated by Eberl and Velde (1989), and checked by data obtained from WINFIT computer program.

The d_{060} values of illite were measured for estimating octahedral Fe + Mg contents (atoms per formula unit, a.p.f.u.) of illites by using the equation of Guidotti et al. (1992). Illite polytypes were identified at characteristic peaks ($2\theta = 16$ –36° CuK α) for un-oriented preparations (Bailey, 1988). Peak area ratios $A_{(2.80\text{\AA})} / A_{(2.58\text{\AA})}$ and $A_{(3.07\text{\AA})} / A_{(2.58\text{\AA})}$, proposed by Grathoff and Moore (1996), were used to evaluate polytype ratios.

The SEM-energy dispersive spectroscopy (EDX) studies were performed using a Quanta 400F Field Emission instrument in Middle East Technical University and Carl Zeiss Supra 40 VP instruments in Pamukkale University in order to determine the particle morphologies and textural relationships. Operating conditions arranged as 32 s counting time and 20 kV accelerating voltage. Additionally, chemical data were obtained by EDX.

Whole rock (16) and monomineralic clay (10) analysis for major and trace elements were carried out by lithium borate fusion Inductively Coupled Plasma-Mass Spectrometry (ICP-MS) at the ACME Labs. 0.2 g of rock powder was fused with 1.5 g LiBO₂ and then dissolved in 100MM3 5% HNO₃. The REE (rare earth element) contents were determined by ICP-MS from pulps after 0.25 g rock-powder was dissolved with 4 acid digestions. Analytical precisions vary from 0.1% to 0.04% for major elements; from 0.1 to 0.5 ppm for trace elements; and from 0.01 to 0.5 ppm for rare earth elements. Trace element contents of 6

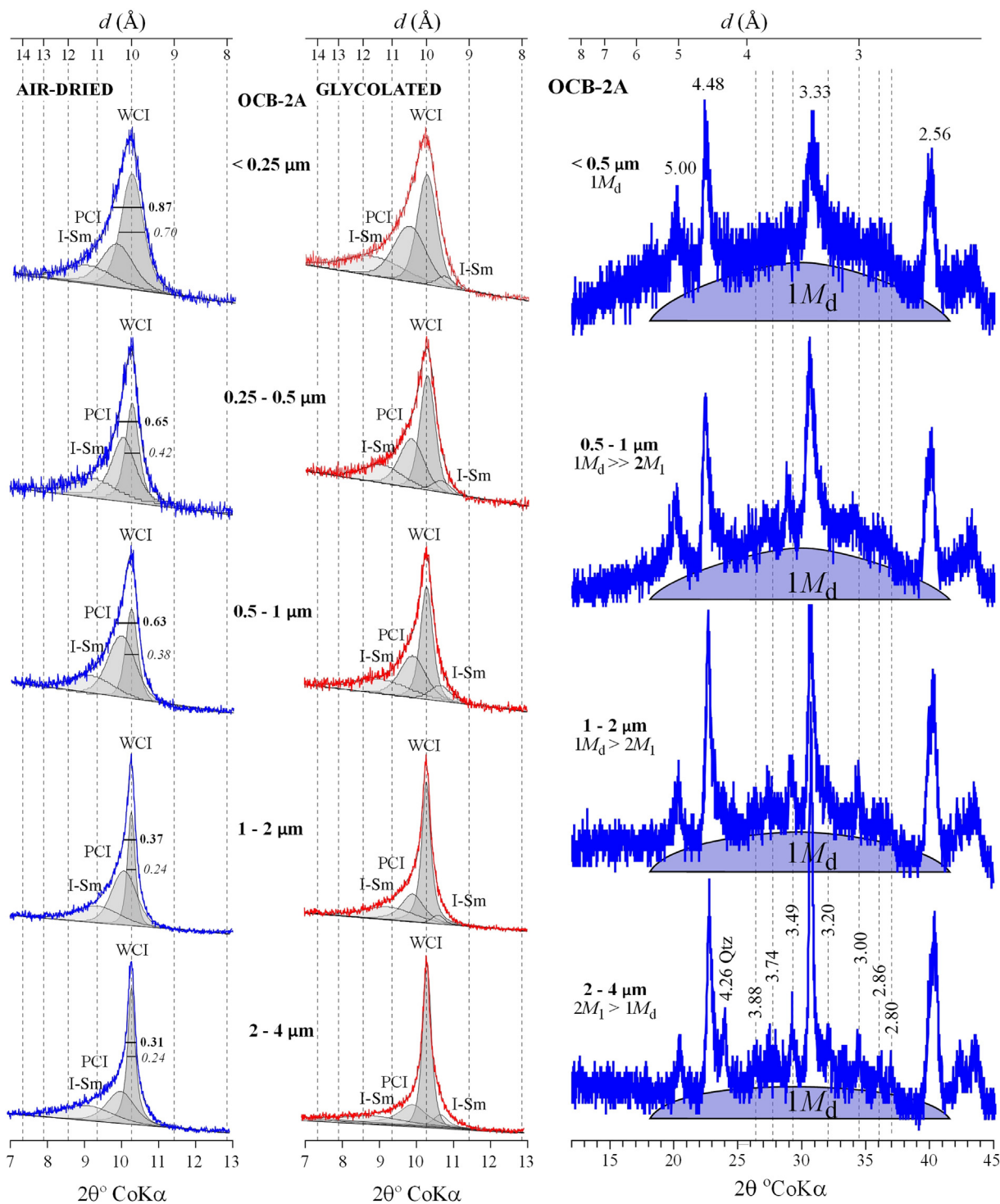


Fig. 7. Decompositions of first order peaks and polytypes of illites based on their different size fractions.

clay samples were performed by ICP-MS at the University of Georgia. The samples digested in 0.125 ml nitric acid and 0.375 ml HCl overnight, with 5 ml HF the following day samples were then microwaved at 400 W for 30 min in sealed teflon containers, and taken up with 32 ml saturated boric acid solvation.

For oxygen isotope analyses, the kaolinite standard (KGA-1) was run with illite samples with a standard deviation of 0.13‰ ($n = 5$). Silicate oxygen analyses were performed by a method modified from Valley et al. (1995), using a garnet standard for oxygen isotope ratios. Samples

(2–3 mg) were reacted under vacuum with BrF₅ while heated with a variable power CO₂ laser (Synrad, 10,510–10,650 nm wavelengths, 75 W max power). Generated O₂ was converted to CO₂ with heated graphite, and the CO₂ was analyzed on a Finnigan MAT 252 mass spectrometer. Sample analyses each day were accompanied by standard mineral analyses. Sample results are adjusted according to the daily average of standard results.

Hydrogen isotope analyses were performed by a method modified from Vennemann and O'Neil (1993), a simple method of

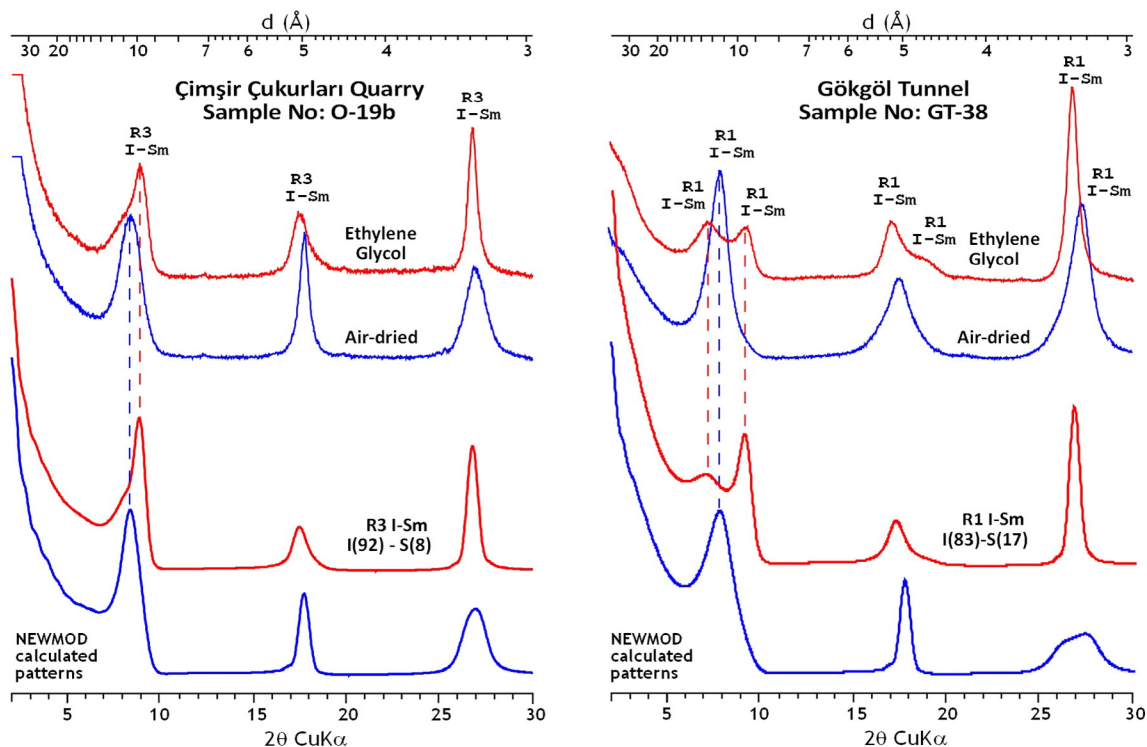


Fig. 8. Experimental and NEWMOD© calculated XRD patterns R1 and R3 ordering types of I-Sm and illite proportions in K-bentonites from Çimşir Çukurları and Gökgöl tunnel section.

Table 2
Crystal-chemical characteristics of illite and I-Sm in K-bentonites.

	KI ($\Delta^{\circ}2\theta$)*	$I(002)/I(001)$	Ir**	d_{060} (\AA)	$2M_1$	$1M_d$
Yılanlı Burnu quarry	0.38–0.78 (0.58)	0.32–0.48 (0.41)	1.13–2.21 (1.47)	1.4992–1.5039 (1.5012)	15–35 25	60–80 75
Gavurpınarı quarry	0.52–0.88 (0.66)	0.38–0.70 (0.49)	1.26–1.99 (1.54)	1.4991–1.5015 (1.5000)	25–35 (32)	65–75 (68)
Çukurören village	0.65–0.92 (0.78)	0.45–0.87 (0.65)	1.71–2.18 (1.95)	1.5000	40	60
Şapçı quarry	1.24–1.27 (1.26)	0.77–0.85 (0.81)	2.14–2.55 (2.35)	1.4967–1.4972 (1.4970)	–	100
Gökgöl tunnel	1.09–1.52 (1.33)	0.33–0.82 (0.59)	2.91–3.81 (3.42)	1.4987–1.4989 (1.4988)	–	100

* KI values reflect re-calibrated CIS-KI values to Basel KI values by using Warr and Ferreiro-Mählemann (2015) equation.

** The interval and mean values of Ir for Yılanlı Burnu and Gavurpınarı quarries reflect somewhat different values than those of Günal-Türkmenoğlu et al. (2015) because of addition of a few samples and repetition of XRD operation for some samples.

hydrogen isotope of minerals and rocks based on zinc reagent. Samples were dehydrated by heating with a gas/oxygen torch under vacuum. Enough sample mass was used to produce 0.5–2 μl

of water (depending on the mineral). Generated water was collected in Pyrex tubes containing zinc granules. Water and zinc were reacted in the sealed tubes at 500 °C to produce H₂ gas and analyzed on mass

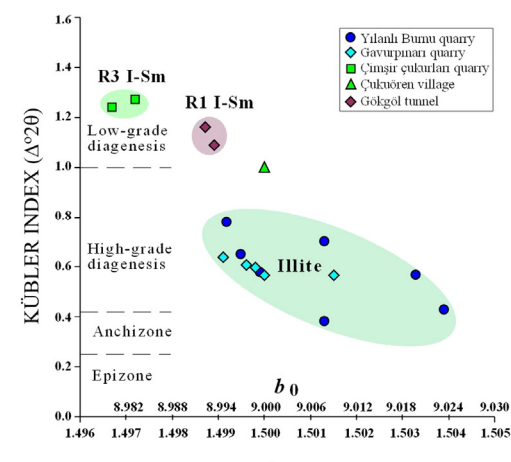
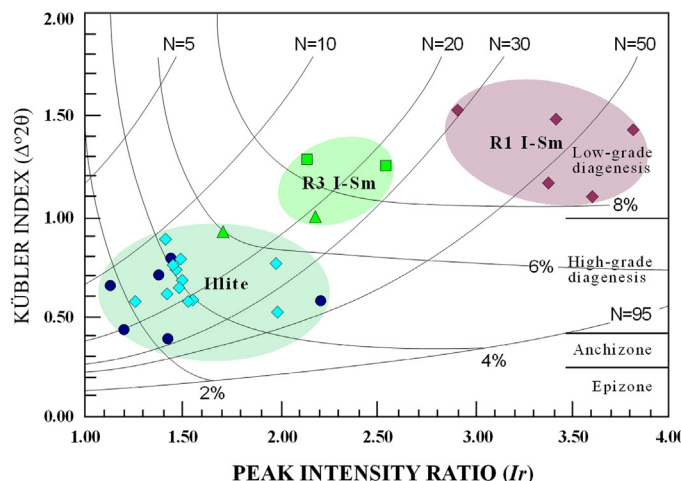


Fig. 9. Diagenetic grade, smectite contents and mean XRD scattering domain sizes of illites on KI vs. Ir diagram of Eberl and Velde (1989) (left), (b) KI vs. d_{060} diagram of illites and I-Sm in K-bentonites.

spectrometer. Analyses of each batch of mineral water samples were accompanied by standard reference waters (V-SMOW and SLAP) reacted with zinc under the same conditions as the samples. Sample isotopic results are normalized to the water standard results using a two-point scale and all δD values are reported relative to V-SMOW. For clay mineral preparation, the 2-sigma of the extraction + analysis is 5% for δD .

K-Ar age determinations on illites and I-Sm were done at the Department of Geosciences, Georgia State University, Atlanta, Georgia, USA. The measurements followed the procedures outlined by De Man et al., 2010. Analytical errors of potassium and radiogenic argon contents are given at the 95% confidence level (2σ). For each K-Ar age determination, a single test portion was used for both the argon isotopic analysis and the potassium determination. Using a single test portion eliminates the effect of weighing error on the K-Ar age value. Ar/Ar age determinations for two samples were made at Earth and Environmental Sciences, University of Michigan, USA. The procedures of Dong et al. (1995) followed for analysis.

4. Results

4.1. Optical microscopy

The K-bentonite samples collected from the Gavurpinarı quarry were studied by optical microscopy. The relict primary volcanogenic minerals are biotite, zircon, quartz, feldspar, amphibole and apatite. Biotite and zircon crystals display euhedral to anhedral crystal outlines. The vitroclastic pyroclastic texture including completely sericitized (illitized) volcanic matrix, volcanic glass and/or pumice shards (Fig. 3a, b; Göncüoğlu et al., 2016), the presence of euhedral zircon crystals (Fig. 3c, d; Göncüoğlu et al., 2016) and volcanogenic biotites (Günal-Türkmenoğlu et al., 2015) indicates the volcanic origin for K-bentonites. Pyrite, dolomite, gypsum and calcite formed as diagenetic minerals. Pyrite is mostly oxidized to goethite that resulted in the yellowish-brown colors of K-bentonites in field exposures.

4.2. Electron microscopy

Illite in the K-bentonites from the Gavurpinarı and Yılanlı Burnu quarries exhibit a platy habit with curved edges (Fig. 4a–c). Nadeau et al. (1985); Inoue et al. (1990) and Altaner and Ylagan (1997) stated that this kind of platy morphology with anhedral flakes is a common feature for illites from K-bentonites. By increasing the proportion of illite layers in mixed-layer I-Sm, the morphology of illite changes from sponge-like or cellular to platy or ribbon-like as a result of a change in layer stacking from turbostratic (randomly distributed layers in any direction) to rotational ordering of the $1M_d$ type during burial diagenesis. This rotational ordered structure results in a plate or sheet-like crystal habit by means of contiguity of quasi-hexagonal oxygen surfaces from adjacent layers, which allows more crystalline regularity in the direction of a - b plane (Keller et al., 1986).

Size fractions of $<0.1 \mu\text{m}$ clay illite from K-bentonite samples from two different locations were investigated by high-resolution transmission electron microscopy (HR-TEM, Günal-Türkmenoğlu et al., 2015). On HR-TEM observations the regular stacking sequence of illites could be observed (Fig. 4d). It is suggested that the illite mineral can be a long-range ordered ($\geq R3$) mixed-layer illite-smectite on the basis of change from random (R0) to short-range (R1) ordered, and then to long-range (R3) ordered I-Sm during progressive illitization of smectite (e.g., Bethke et al., 1986; Lindgreen and Hansen, 1991). Illite crystals exhibit anhedral lamellar micro morphologies and ordered lattice fringe images with T-O-T layers (Fig. 4d). This kind of ordered structure with few defects, demonstrates an effect of advanced stage of diagenetic evolution on the studied illites (Merriman and Peacor, 1999). The crystallite

sizes of illite particles reach up to 20 nm that is compatible with data obtained from KI-Ir diagram (see Fig. 9a).

4.3. Mineralogy

K-bentonites contain mainly calcite, dolomite, quartz, feldspar and clay minerals (Table 1). Trace amounts of pyrite, goethite, gypsum, anatase, and jarosite were also found in the K-bentonite samples. Illite is the major clay mineral in the K-bentonite samples from the Gavurpinarı and Yılanlı Burnu quarries, whereas R3 and R1 I-Sm dominate in K-bentonite samples from the Çimşir Çukurları quarry and the Gökgöl tunnel, respectively (see Fig. 5). In a few samples, trace amount of kaolinite and imogolite are also identified (Günal-Türkmenoğlu et al., 2015). Illites have typical sharp peaks at 10 Å (001), 5 Å (002) and 3.33 Å (003)

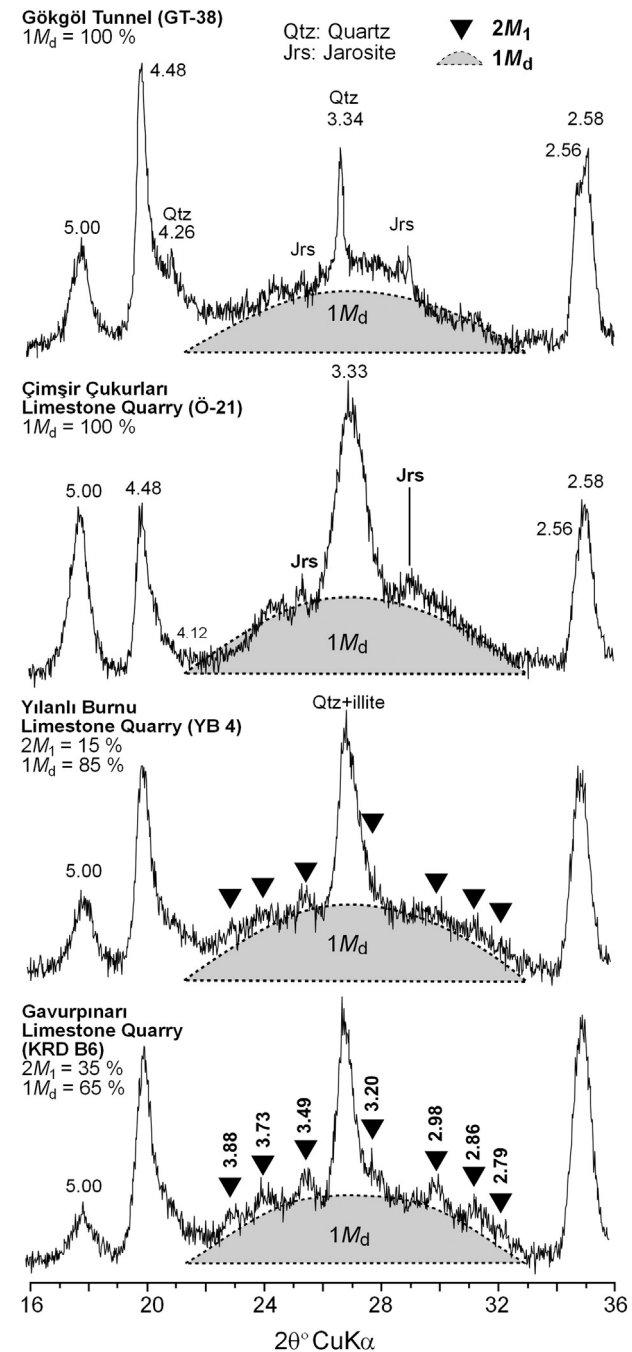


Fig. 10. Unoriented powder diffraction patterns of polytypes from the illite and I-Sm in K-bentonites.

indicating pure phase, but the deconvolution of asymmetric peaks show the presence of three phases as well crystallized illite (WCI), poorly crystallized illite (PCI), and lesser amounts of mixed-layer illite-smectite (I-Sm) (Fig. 6). Together with the increasing grain sizes from 0.25 µm to 2 µm, the PCI and WCI peaks relatively sharpen and become narrower (Fig. 7).

XRD patterns of I-Sm of K-bentonites from the Çimşir Çukurları quarry and Gökgöl Tunnel sections indicate R3 and R1 ordering types, respectively. The illite proportions in R3 and R1 I-Sm, calculated from the data of Moore and Reynolds (1997), are determined to be 92% and 83%. NEWMOD©-calculated patterns of I-Sm demonstrate the same values (Fig. 8).

The KI values of illites range from 0.38 to 0.78 (an average of 0.58 Δ°20) for the Gavurpinarı quarry, and from 0.52 to 0.88 (an average of 0.66 Δ°20) for the Yılanlı Burnu quarry that indicate high diagenetic grade (Table 2 and Fig. 9a, b). KI values of illite/I-Sm minerals in K-bentonites from Çimşir Çukurları and Gökgöl Tunnel represent low-grade diagenetic conditions.

The Ir values (1.26–1.99, an average of 1.54 for the Gavurpinarı quarry, 1.13–2.21 an average of 1.47 for the Yılanlı Burnu quarry) point out the presence of swelling layers (smectite) in illites. Thus, Ir values of Gavurpinarı illites display higher values than Yılanlı Burnu quarry illites that can be explained by relatively higher smectite contents and lower diagenetic conditions. The comparison of KI and Ir of illites illustrates that the content of swelling (or smectite) component and mean XRD scattering domain size (N) of illites are 2–5% and 10–25 nm, respectively (Fig. 9a).

K-bentonites that are illite-rich (i.e., no I-Sm), polytypes are represented by 2M₁ and 1M_d, whereas K-bentonites with mixed layer clays (i.e., R3 and R1 I-Sm) exhibit only 1M_d (Fig. 10). 2M₁/(2M₁ + 1M_d) ratios (%) are more or less similar (15–35%, an average of 28%) for two quarries in Bartın area. However illites of the Gavurpinarı quarry have higher fractions of 2M₁ than illites of the Yılanlı Burnu quarry (Table 2). 1M_d ratio increases together with the decreasing grain-size and represent completely 1M_d in <0.5 µm fraction (see Fig. 7).

The d₀₆₀ values of illites from the Yılanlı Burnu and Gavurpinarı quarry samples range from 1.4991 to 1.5039 Å indicating compositions between ideal muscovite and phengite (i.e., octahedral Mg + Fe = 0.08–0.61 a.p.f.u.). Smaller d₀₆₀ values were obtained from the Yılanlı Burnu quarry dominated by dolomitic rocks, where values of Çimşir Çukurları quarry and Gökgöl Tunnel range from 1.4967–1.4989 Å, thus indicating muscovitic composition (i.e., octahedral Mg + Fe < 0.06 a.p.f.u.). The estimation of octahedral Fe + Mg contents from d₀₆₀ values can be incompatible with the values derived from chemical analyses, however the differences in d₀₆₀ values may be useful for relative characteristics of K-bentonites.

4.4. Geochemistry

4.4.1. Major element geochemistry and structural formula

The major element composition of illite and I-Sm and their structural formulas (based on 22 negative charges matched to 10 oxide and 2 hydroxide ions, Weaver and Pollard, 1973) are given in Table 3. Illite IV^{Al} substitutions range from 0.37–0.56 atoms for the Gavurpinarı quarry and 0.32–0.34 for the Yılanlı Burnu quarry. Illite octahedral compositions of the Gavurpinarı and Yılanlı Burnu quarries range 0.06–0.50 for VI^{Fe²⁺}, 0.31–0.63 for VI^{Mg}, and 1.30–1.60 for VI^{Al}, respectively. I-Sm minerals are characterized by relatively higher amounts of tetrahedral Al for Si substitution (0.44–0.65), lower octahedral substitutions for VI^{Fe²⁺} (0.03–0.24) and for VI^{Mg} (0.25–0.54), and higher for VI^{Al} (1.44–1.75) compared to those of illites. The major interlayer cation (K⁺) has similar stoichiometric values for illite (0.51–0.66 atoms) and I-Sm (0.56–0.68 atoms), but Ca²⁺ is slightly higher for I-Sm. Samples from all areas fall both within the area of illite and I-Sm in the tetrahedral charge versus octahedral charge ternary diagram (Fig. 11a). Illites from the K-bentonites in the Gavurpinarı and Yılanlı Burnu quarries were distinguished by their tetrahedral charge as seen on a – M⁺, 4Si, R²⁺ – ternary diagram (Fig. 11b). In the Si versus Na + K compositional diagram, samples fall below the illite point and they may be distinguished on the basis of their Si and interlayer cation contents

Table 3
Major oxide element compositions and structural formulas of illites and I-Sm in K-bentonites.

Oksit %	Gavurpinarı Quarry							Yılanlı Burnu Quarry			Ç.Ören		Çimşir Çukurları		Gökgöl Tunnel		
	OCB-1	OCB-2A	KRD-B6	09YB4	KRD-B2	KRD-B3	KRD-B7	YBA-19A	YBA-10	YB-4	Ö-17A	Ö-19	Ö-21	GT-3	GT-31	GT-38	
SiO ₂	51.22	54.34	54.12	51.27	49.19	48.54	51.10	56.33	55.18	55.21	52.63	49.93	50.43	50.16	49.34	50.27	
TiO ₂	0.815	1.184	0.936	1.200	1.000	0.96	1.09	0.441	0.663	0.566	0.52	0.93	0.94	1.00	0.53	0.49	
Al ₂ O ₃	26.83	24.99	25.57	24.26	23.85	22.38	25.74	24.70	20.83	20.65	21.66	28.36	27.13	23.12	25.44	25.06	
ΣFeO	3.62	1.93	2.47	2.38	5.42	8.31	1.81	1.18	4.21	2.91	3.30	0.44	0.76	4.06	2.21	1.97	
MnO	0.000	0.061	0.082	0.01	0.01	0.01	0.01	0.033	0.027	0.007	0.01	0.01	0.01	0.02	0.01	0.01	
MgO	4.50	3.15	3.97	3.35	3.03	3.09	3.32	4.66	6.29	6.39	4.34	2.45	2.80	2.78	5.24	4.93	
CaO	0.14	0.17	0.55	0.50	0.49	0.17	0.87	0.06	0.32	1.18	0.82	0.65	0.75	1.31	1.10	1.03	
Na ₂ O	0.26	0.19	0.40	0.39	0.27	0.50	0.16	0.36	0.13	0.12	0.11	0.12	0.05	0.08	0.02	0.02	
K ₂ O	5.93	7.78	7.68	7.13	6.96	6.61	7.32	6.09	7.62	7.44	6.61	7.40	7.33	7.64	6.82	6.41	
P ₂ O ₅	0.21	n.a.	0.64	0.56	0.33	0.36	0.39	0.25	0.16	0.13	0.06	0.09	0.05	0.04	0.01	0.01	
LOI	6.98	6.85	6.00	9.00	8.60	7.90	8.00	6.98	6.18	6.45	9.40	8.90	9.40	9.51	9.02	9.53	
Toplam	100.51	100.65	102.42	100.05	99.15	98.83	99.81	101.08	101.61	101.05	99.46	99.28	99.65	99.72	99.74	99.73	
Si ^{IV}	3.44	3.63	3.56	3.57	3.49	3.49	3.51	3.68	3.67	3.68	3.66	3.44	3.49	3.56	3.42	3.48	
Al ^{IV}	0.56	0.37	0.44	0.43	0.51	0.51	0.49	0.32	0.33	0.32	0.34	0.56	0.51	0.44	0.58	0.52	
TC	0.56	0.37	0.44	0.43	0.51	0.51	0.49	0.32	0.33	0.32	0.34	0.56	0.51	0.44	0.58	0.52	
Al ^{VI}	1.56	1.60	1.54	1.56	1.49	1.38	1.60	1.57	1.30	1.30	1.44	1.75	1.69	1.49	1.49	1.52	
Fe ^{+2VI}	0.20	0.11	0.14	0.14	0.32	0.50	0.10	0.06	0.23	0.16	0.19	0.03	0.04	0.24	0.13	0.11	
Mg ^{VI}	0.45	0.31	0.39	0.35	0.32	0.33	0.34	0.45	0.62	0.63	0.45	0.25	0.29	0.29	0.54	0.51	
TOC	2.22	2.03	2.07	2.05	2.14	2.21	2.05	2.09	2.16	2.10	2.08	2.02	2.03	2.03	2.16	2.14	
OC	0.00	0.34	0.33	0.33	0.24	0.19	0.31	0.24	0.38	0.50	0.39	0.20	0.25	0.46	0.18	0.20	
Ca	0.01	0.01	0.04	0.04	0.04	0.01	0.06	0.00	0.02	0.08	0.06	0.05	0.06	0.10	0.08	0.08	
Na	0.03	0.02	0.05	0.05	0.04	0.07	0.02	0.05	0.02	0.02	0.01	0.02	0.01	0.01	0.00	0.00	
K	0.51	0.66	0.64	0.63	0.63	0.61	0.64	0.51	0.65	0.63	0.59	0.65	0.65	0.69	0.60	0.57	
ILC	0.56	0.71	0.77	0.76	0.74	0.70	0.79	0.56	0.71	0.82	0.72	0.76	0.76	0.90	0.77	0.72	
TLC	0.56	0.71	0.77	0.76	0.74	0.70	0.79	0.56	0.71	0.82	0.72	0.76	0.76	0.90	0.77	0.72	

ΣFeO: total iron, TC: tetrahedral charge, TOC: total octahedral cations, OC: octahedral charge, ILC: interlayer cations, TLC: total layer charge.

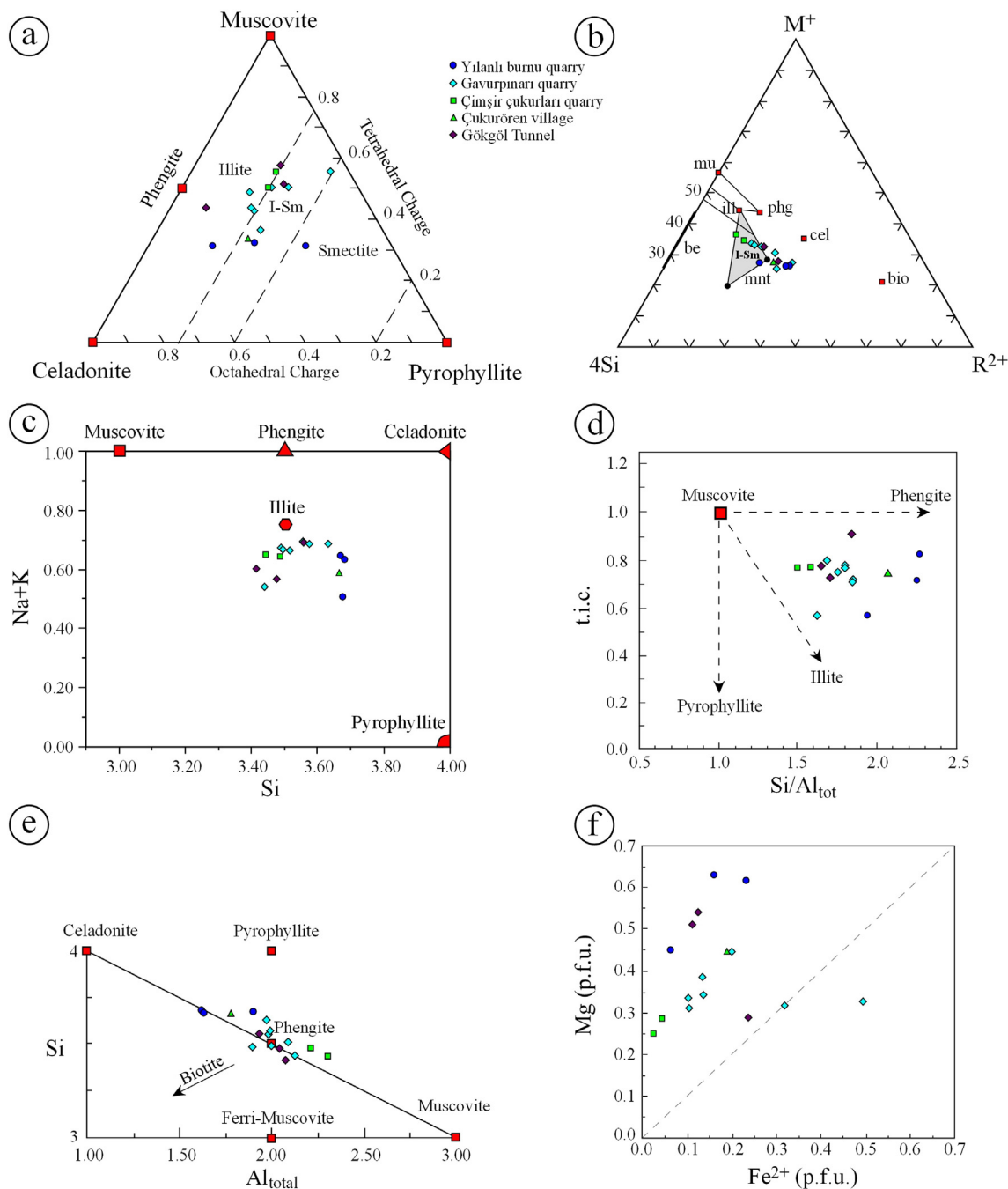


Fig. 11. Compositional diagrams based on the structural formulas of illites and I-Sm in K-bentonites. (a) Muscovite-Pyrophyllite-Celadonite, (b) $M^+-R^{2+}-4Si$, (c) $Na + K$ vs. Si, (d) total interlayer cations (t.i.c.) vs. Si/Al_{tot} , (e) Si vs. Al_{tot} , (f) Mg vs. Fe.

(Fig. 11c). In the total interlayer cations (t.i.c.) versus Si/Al_{tot} and Si versus Al_{tot} diagrams, illite and I-Sm have phengitic compositions (Fig. 11d, e). Mg is the dominant octahedral cation rather than Fe (Fig. 11f), suggesting that Mg diffusion from dolomitic host rocks may have occurred.

4.4.2. Trace element and REE geochemistry

The trace element concentrations of illites and I-Sm differ from each other (Table 4). The mean values of the transition metals, except for Pb and Zn, and large-ion lithophile elements (LILE) are higher in illites of the Yılanlı Burnu and Gavurpinarı quarries, whereas high-field-strength elements (HFSE) contents, except for Ta, are

higher in the I-Sm of Çimşir Çukurları quarry and Gökgöl tunnel. The elements with the lowest concentrations within the clay minerals are Bi, In, Mo, Sb, Ag and Tl.

Chondrite-normalized (Sun and McDonough, 1989) values of some trace elements and REEs (Fig. 12) illustrate that the content of trace elements increases in I-Sm, except for Rb, Ba, Ta, Sr and P, and their patterns appear to show significant dissimilarity from each other and the North American Shale Composite (NASC: Nb and Y from Condé, 1993; other elements from Gromet et al., 1984). Chondrite-normalized REE patterns of illites and I-Sm are distinguishable from one another and display clear fractionation (Fig. 13). I-Sm minerals from Çimşir Çukurları quarry and Gökgöl tunnel section have higher REE values than those of

Table 4

Trace element compositions of illites and I-Sm in K-bentonites.

Element	Gavurpinarı Quarry					Yılanlı Burnu Quarry			Çören	Çimşir Çukurları		Gökgöl Tunnel			
	OCB-1	KRD-B6	09YB4	KRD-B2	KRD-B3	KRD-B7	YBA-19A	YBA-10	YB-4	Ö-17A	Ö-19	Ö-21	GT-3	GT-31	GT-38
				Illite	Illite	Illite	Illite	Illite	Illite	R3 I-Sm	R1 I-Sm				
Cr	107.68	117.85	130.00	123.00	123.00	144.00	141.26	107.28	104.96	116.00	55.00	62.00	21.00	14.00	14.00
Ni	36.24	11.33	43.00	26.00	65.00	8.50	27.93	32.24	33.70	24.00	11.90	20.00	10.70	1.80	0.40
Co	10.78	4.46	13.00	4.80	13.40	3.70	5.91	4.72	3.84	6.20	0.80	1.10	0.70	0.30	0.20
Sc	n.a.	n.a.	19.00	13.00	16.00	16.00	n.a.	n.a.	n.a.	18.00	14.00	4.00	n.a.	n.a.	n.a.
V	175.39	220.64	157.00	201.00	203.00	190.00	163.02	130.91	143.18	135.00	323.00	289.00	68.00	13.00	8.00
Cu	14.07	5.23	n.a.	n.a.	n.a.	6.60	10.98	17.51	19.26	15.50	n.a.	1.80	5.40	1.80	1.50
Pb	39.82	24.34	n.a.	n.a.	n.a.	1.50	8.68	20.07	17.03	3.00	n.a.	1.50	16.30	70.20	88.20
Zn	158.02	92.36	n.a.	n.a.	n.a.	43.00	24.01	52.87	55.23	20.00	n.a.	29.00	177	110	79
Bi	<0.45	<0.45	n.a.	n.a.	n.a.	0.10	<0.45	<0.45	<0.45	0.10	n.a.	0.10	0.10	0.20	0.20
In	<0.1	<0.1	n.a.	n.a.	n.a.	n.a.	0.113	<0.1	<0.1	n.a.	n.a.	n.a.	n.a.	n.a.	n.a.
Sn	7.4	6.74	3.00	3.00	4.00	7.09	1.06	6.41	3.00	8.00	2.00	3.00	5.00	4.00	
W	6.32	9.53	5.70	12.20	4.80	8.80	6.45	0.26	2.71	16.60	19.30	9.70	2.20	1.70	1.00
Mo	1.72	0.93	n.a.	n.a.	n.a.	0.10	6.86	2.13	2.22	0.10	n.a.	0.10	6.50	12.10	14.80
As	42.54	11.63	n.a.	n.a.	n.a.	1.30	3.71	13.17	16.70	3.00	n.a.	1.90	36.70	33.40	14.80
Sb	3.92	1.62	n.a.	n.a.	n.a.	0.10	0.59	0.75	0.45	0.10	n.a.	0.10	4.60	0.30	0.10
Ge	2.64	1.44	n.a.	n.a.	n.a.	2.17	0.39	1.48	n.a.	n.a.	n.a.	n.a.	n.a.	n.a.	n.a.
Be	5.61	5.34	4.00	4.00	5.00	4.00	4.62	5.11	4.38	6.00	3.00	4.00	3.00	4.00	3.00
Ag	20.14	19.16	n.a.	n.a.	n.a.	0.10	<1.00	<1.00	<1.00	0.10	n.a.	0.10	1.00	1.00	1.00
Rb	265.65	234.29	275.80	270.20	254.50	302.60	268.68	298.48	288.03	319.00	167.50	189.60	124.70	151.80	159.30
Cs	23.10	17.27	17.80	15.20	19.50	30.60	17.91	24.68	21.82	39.50	18.60	25.30	17.30	21.00	31.30
Ba	206.65	148.80	269.00	255.00	233.00	310.00	252.60	123.41	105.68	302.00	64.00	35.00	66.00	20.00	19.00
Sr	373.35	254.84	888.20	749.20	350.70	759.50	800.79	491.97	182.38	38.70	232.00	42.20	40.80	30.90	19.60
Tl	0.87	0.92	n.a.	n.a.	n.a.	0.10	3.42	2.28	2.05	0.90	n.a.	0.80	2.27	0.05	0.01
Ga	n.a.	n.a.	28.2	31.1	24.9	28.2	n.a.	n.a.	26.3	29.3	28.8	22.90	41.70	47.20	
Ta	39.40	97.15	1.70	1.50	1.60	1.60	39.41	8.45	35.62	0.80	17.00	4.40	15.30	9.90	10.70
Nb	32.82	32.84	26.70	21.30	20.70	22.70	24.90	2.40	17.22	10.00	308.60	180.40	206.70	155.00	163.70
Hf	6.65	7.66	4.60	3.90	4.20	4.80	2.31	0.42	3.75	1.30	68.10	23.50	18.60	30.00	33.00
Zr	358.28	424.73	178.20	149.80	146.80	170.80	139.15	24.21	219.78	45.30	2550.80	1108.00	764.00	917.10	968.40
Y	8.25	8.42	16.40	6.60	10.70	15.40	100.95	22.00	21.76	7.00	182.00	57.10	47.60	14.90	15.50
Th	1.39	6.48	14.70	10.50	9.60	18.80	6.19	37.74	14.62	7.70	80.70	37.80	16.30	38.20	45.60
U	9.24	8.55	8.90	8.10	9.10	7.80	3.85	7.72	5.51	2.00	43.60	30.90	7.10	1.20	1.70
La	7.07	10.96	45.20	24.90	31.60	30.90	36.21	24.92	19.11	17.70	200.30	38.90	117.40	5.10	8.00
Ce	44.46	37.63	93.00	42.80	63.50	62.40	69.51	41.19	32.39	36.70	393.10	46.50	247.30	15.60	23.20
Pr	2.19	2.22	10.99	4.47	7.09	6.95	6.93	4.23	3.09	3.72	43.19	5.69	31.59	2.86	4.04
Nd	8.20	6.88	38.00	14.50	22.40	23.80	20.78	14.71	10.01	12.30	129.90	20.90	110.2	12.80	18.60
Sm	1.35	1.05	5.26	1.68	3.06	3.93	1.51	2.03	1.21	2.32	32.33	5.69	18.24	3.22	4.09
Eu	0.29	0.22	0.94	0.31	0.51	0.76	0.23	0.33	0.21	0.39	5.67	1.60	3.31	0.38	0.42
Gd	1.39	1.10	3.63	1.16	2.11	3.07	1.31	1.47	1.06	1.76	31.01	6.92	13.39	2.61	3.11
Tb	0.20	0.17	0.56	0.18	0.33	0.52	0.14	0.22	0.15	0.28	5.82	1.08	1.79	0.49	0.53
Dy	1.36	1.23	3.08	1.20	2.10	3.07	0.90	1.43	0.94	1.60	34.89	6.30	9.02	2.98	2.72
Ho	0.28	0.28	0.61	0.28	0.43	0.57	0.19	0.31	0.20	0.30	6.15	1.27	1.55	0.60	0.48
Er	0.97	0.98	2.00	1.01	1.39	1.77	0.77	0.99	0.70	0.88	17.17	3.63	3.89	1.76	1.36
Tm	0.17	0.17	0.32	0.17	0.25	0.30	0.13	0.15	0.12	0.15	2.41	0.48	0.55	0.26	0.21
Yb	1.25	1.31	2.25	1.17	1.75	2.08	1.10	1.17	0.88	1.11	14.29	2.90	3.44	1.83	1.43
Lu	0.20	0.20	0.35	0.20	0.28	0.30	0.17	0.17	0.13	0.16	2.00	0.40	0.50	0.27	0.21

illites from the Yılanlı Burnu and Gavurpinarı quarries. In general, patterns exhibit similar trends, and light REE (LREE) concentrations are enriched with respect to high REE (HREE). All of the clays exhibit clear

enrichment with respect to the chondrite. Some I-Sm minerals are enriched, but illites are depleted with respect to NASC. The clays have negative Eu and positive Gd anomalies.

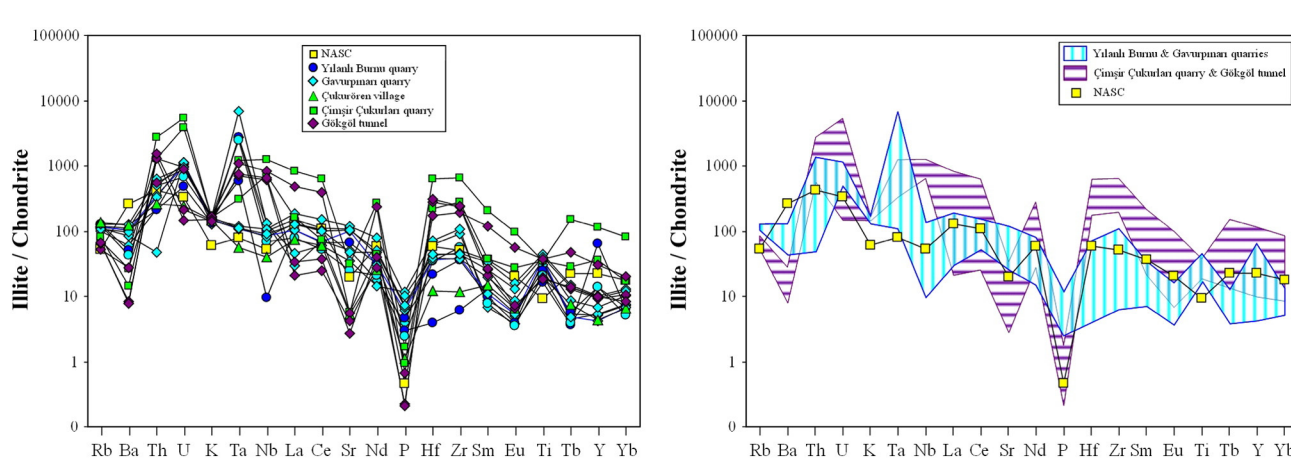


Fig. 12. Chondrite-normalized multiple trace element spider diagram of illites and I-Sm in K-bentonites.

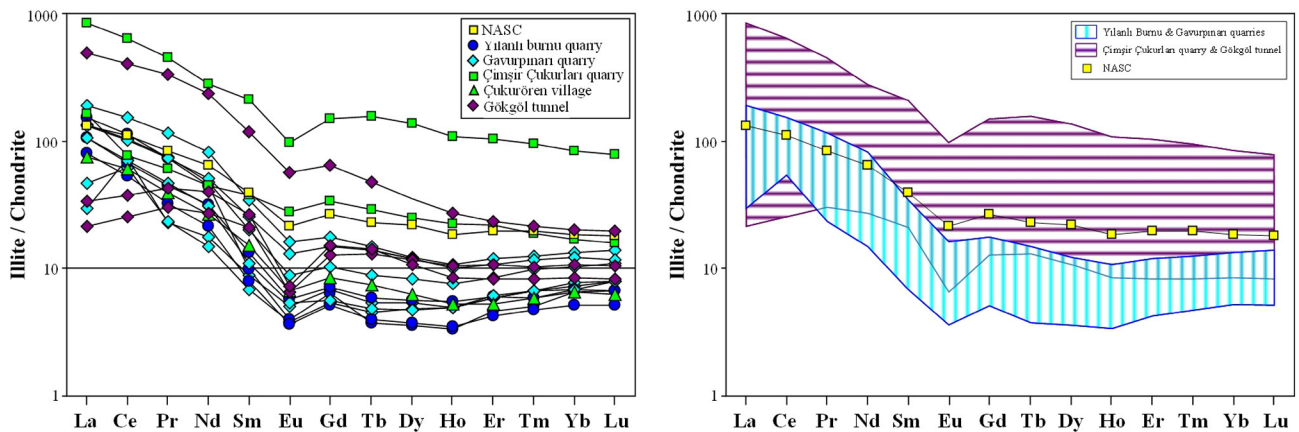


Fig. 13. Chondrite-normalized REE spider diagram of illites and I-Sm in K-bentonites.

Table 5
Oxygen and hydrogen isotope data of illite and I-Sm in K-bentonites.

Sample No	Mineral	$\delta^{18}\text{O}$	δD
Gavurpinarı quarry			
KRD-B6	Illite	18.65	-47.3
OCB-1	Illite	18.13	-22.4
OCB-2A	Illite	17.75	-69.9
Yılanlı Burnu quarry			
YB-4	Illite	19.96	-10.1
YBA-10	Illite	18.87	-34.1
YBA-19A	Illite	20.14	-63.9
Cimşir Çukurları quarry			
Ö-19	R3 I-Sm	21.91	-51.4
Ö-21	R3 I-Sm	21.84	-49.6

4.4.3. Stable isotope geochemistry

Stable isotope compositions of eight pure clay samples show that the $\delta^{18}\text{O}$ values vary in a narrow range from +17.75‰ to 21.91‰ (SMOW), whereas those of δD are distributed over a wide range, -10.1‰ to -69.9‰ (SMOW) (Table 5). The isotope data of the clay minerals are presented in Fig. 14a, together with the meteoric water line (Craig, 1961), supergene-hypogene line for kaolinite (Sheppard et al., 1969), and the line for montmorillonite (Savin and Epstein, 1970). The isotopic composition of the seawater (SW), and meteoric water (Eastern Mediterranean Meteoric Water: EMMW, $\delta^{18}\text{O} = -6.12\text{‰}$, $\delta\text{D} = -37.96\text{‰}$,

Gat et al., 1996) have also been drawn. Illites are in supergene and hypogene areas, whereas I-Sm are supergene area (see Fig. 14a). For the clay-water fractionation equations of Savin and Lee (1988) and Yeh (1980) were used, respectively. The calculated isotopic ratios of fluids in equilibrium with clay–water fractionation factors indicate that the origin of waters reflect a broad range of meteoric and seawater (Fig. 14a), demonstrating the mixture of seawater and meteoric water. For the assumed temperatures of illites (120 °C for Gavurpinarı and 140 °C for Yılanlı Burnu) and I-Sm (80 °C), on the basis of their crystal-chemical data, the isotopic composition of waters fall in metamorphic and magmatic water composition (Fig. 14a, b).

4.4.4. K-Ar and Ar/Ar dating

Assuming that illites in K-bentonite are completely of tephra origin, two Ar/Ar and eight K/Ar analyses were performed on <2 μm illite fractions (Table 6; Fig. 15) with polytypes of $2M_1 + 1M_d$. (see Fig. 7). The K/Ar ages of illites in K-bentonites from the Gavurpinarı and Yılanlı Burnu quarries yield 253–290 Ma. Illite age analysis (Pevear, 1999) was used to check for origin and/or age of $2M_1$ and $1M_d$ illites by examining ages from different size fractions (Table 6; 2–1 μm, 1–0.5 μm and <0.5 μm). The $2M_1$ ratio decreases together with decreasing grain size. Only $1M_d$ forms are found at <0.5 μm size fraction. The age data show that some of $2M_1$ illites may represent inheritance of the older rocks (i.e., they are of detrital origin). We assume the <0.5 μm size fraction directly yielded the illitization (or diagenetic) age. The paleontological data for the deposition of tephras indicate Frasnian (Late Devonian) for Gavurpinarı and Yılanlı Burnu (Günel-Türkmenoğlu et al., 2015;

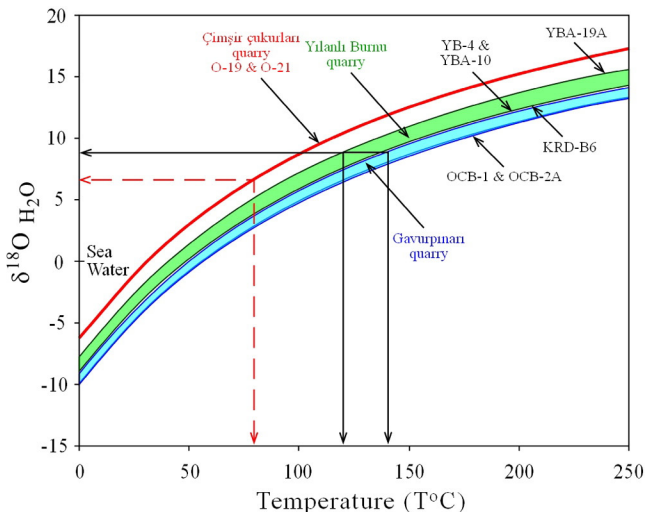
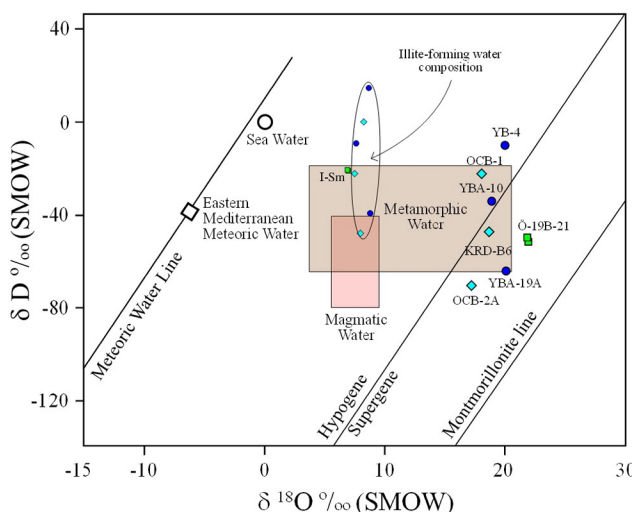
Fig. 14. δD vs. $\delta^{18}\text{O}$ plots of illites and I-Sm (left) and temperature related water compositions.

Table 6

K/Ar analytical data of illite and I-Sm with different size-fractions.

Sample No (grain size)	Mineral	K ₂ O %	⁴⁰ Ar %	⁴⁰ Ar μmol kg ⁻¹	Age (Ma ± 2σ)
Gavurpinarı quarry					
KRD-B6 (<2 μm)	Illite	7.62 ± 0.18	97.2	3.45 ± 0.10	290 ± 7.1
KRD-B7 (<2 μm)	Illite	7.72 ± 0.27	94.9	3.02 ± 0.09	253 ± 4.9
OCB-2A (2–1 μm)	Illite	7.65 ± 0.24	96.6	4.12 ± 0.11	340 ± 5.9
OCB-2A (1–0.5 μm)	Illite	7.58 ± 0.25	96.5	3.83 ± 0.11	321 ± 6.2
OCB-2A (<0.5 μm)	Illite	4.79 ± 0.15	80.3	2.10 ± 0.06	281 ± 4.9
Yılanlı Burnu quarry					
YBA-10 (<2 μm)	Illite	7.49 ± 0.23	95.6	3.63 ± 0.09	309 ± 5.8
YBA-19A (2–1 μm)	Illite	7.80 ± 0.20	96.6	4.17 ± 0.12	337 ± 8.0
YBA-19A (<0.5 μm)	Illite	4.67 ± 0.18	78.3	2.06 ± 0.08	283 ± 5.3
Çimşir Çukurları quarry					
Ö-19 (<2 μm)	R3 I-Sm	7.76 ± 0.22	97.1	2.24 ± 0.06	190 ± 3.1
Ö-21 (<2 μm)	R3 I-Sm	7.65 ± 0.20	97.1	2.13 ± 0.05	184 ± 2.9
Gökgöl Tunnel section					
02DB02 (<2 μm)	R1 I-Sm	6.37 ± 0.17	92.6	1.68 ± 0.04	174 ± 3.0
Güdüllü section					
Ö-17A (<2 μm)	R3 I-Sm	7.07 ± 0.19	96.5	3.40 ± 0.10	307 ± 7.4

Göncüoğlu et al., 2016), whereas illitization ages correspond to the Early Permian period (i.e., approximately 80 Ma after sedimentation) (Fig. 16). The Çimşir Çukurları quarry and Gökgöl Tunnel section have an Early Carboniferous depositional age, and illitization age of tephras as late as Early Jurassic time (approximately 160 Ma after sedimentation).

5. Discussion

5.1. Mineralogy and diagenetic grade of K-bentonites

The degree of illitization in tephras, depends on the composition of the precursor tephra, the water/rock ratio, and the fluid chemical

composition as modified through gains and losses of elements in the altering solutions (Christidis, 1998). During early diagenesis, the homogenization of tephra with marine and meteoric pore waters, volcanic glass progressively alters or transforms into smectite, then mixed-layer illite-smectite, and finally illite.

The studied K-bentonites intercalated with the carbonate rocks of the Late Devonian-Early Carboniferous Yılanlı formation exposed at the Gavurpinarı and Yılanlı Burnu quarries in Bartın area consist mainly of high-grade diagenetic illites, whereas the R3 and R1 mixed-layer illite-smectite in the Çimşir Çukurları quarry and Gökgöl Tunnel section in Zonguldak area are low-diagenetic. The differences in mineralogical composition related to diagenetic grades for Bartın and Zonguldak

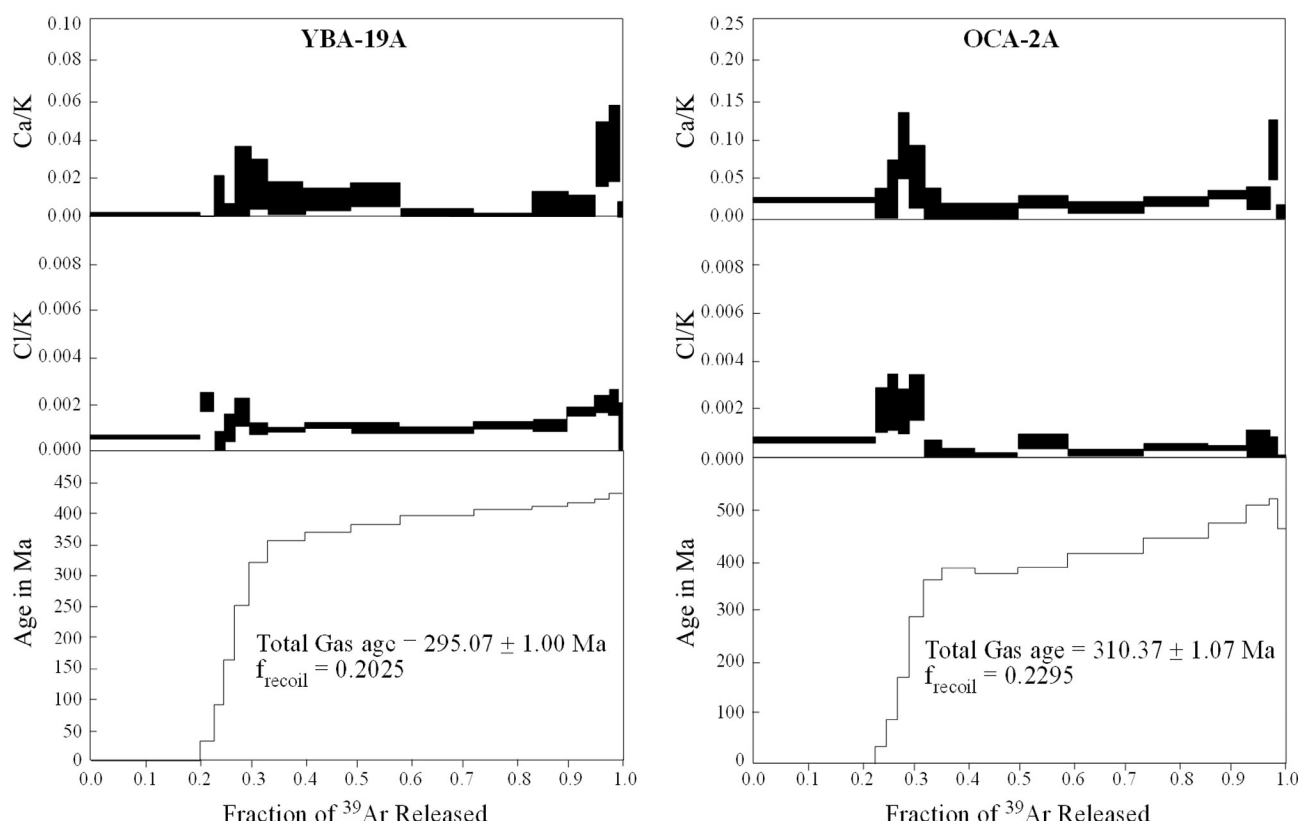


Fig. 15. Ar/Ar dating data of illites (<2 μm size) from Yılanlı Burnu (left) and Gavurpinarı (right) quarries.

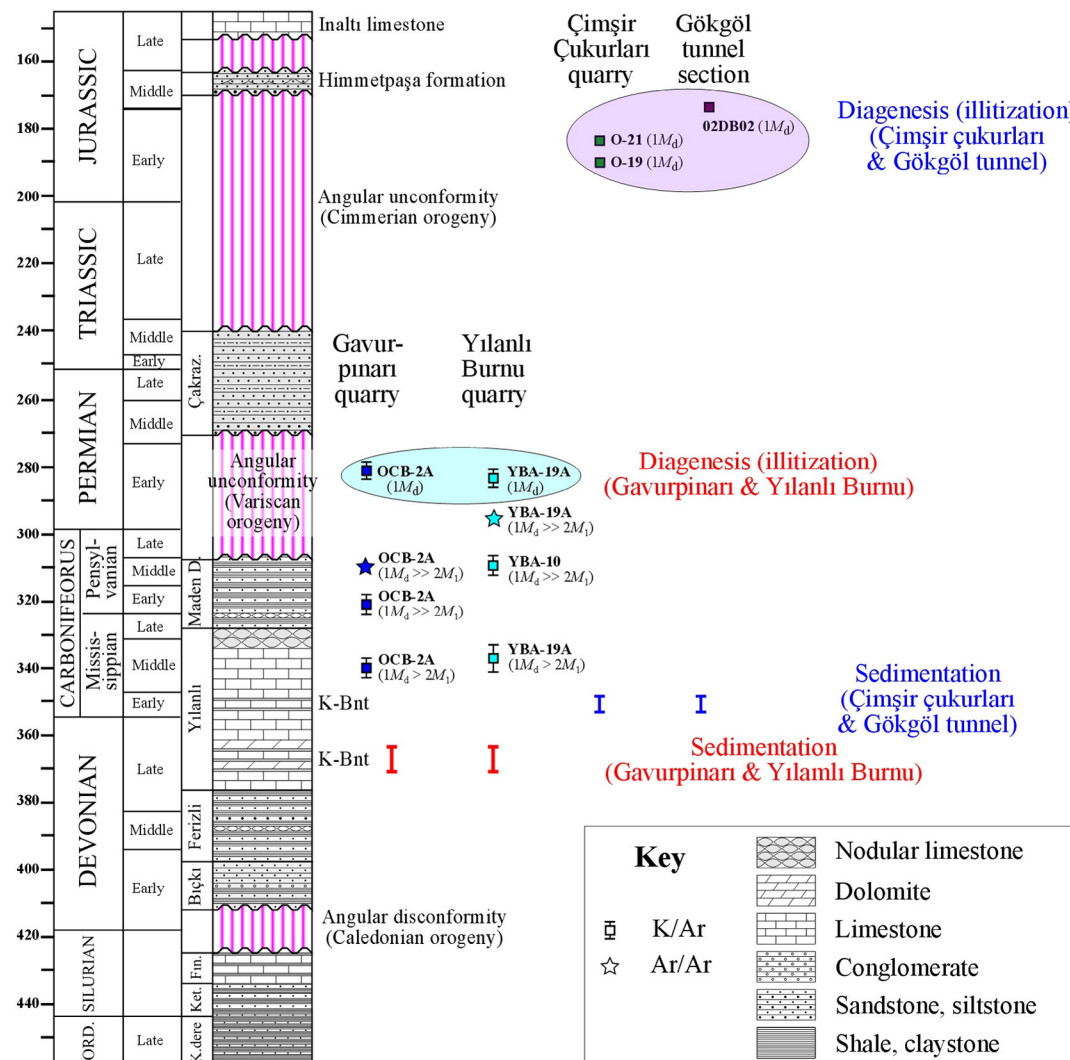


Fig. 16. The position of illitization ages on the generalized section of Zonguldak Terrane.

regions seem to be controlled by the stratigraphic levels (i.e. duration of burial) of tephras. However, they may also relate to different burial histories of these two regions that include maximum depths of burial and temperatures. Thus, ages and relative stratigraphic positions of illite and I-Sm bearing tephra levels must not be the only cause of these differences in diagenetic grades.

Illite polytypes identified for different size fractions showed that fine-grained (<0.5 µm, diagenetic) illites are rich in 1M_d polytypes, whereas coarse-grained (>2 µm) illites are dominated by 2M_i polytype. This finding may be explained in two different ways: (1) increasing grain sizes and 2M_i polytype ratio together with the increasing diagenesis/metamorphism, and (2) presence of coarse-grained 2M_i white K-micas with detrital origin. The mineralogical differences were also encountered in terms of *b* cell dimensions of clays in these two areas, where the *d*₀₆₀ values of illites in the Bartın (Gavurpinari and Yılanlı Burnu) area are somewhat larger than those of I-Sm in the Zonguldak area. The highest *d*₀₆₀ values were particularly obtained from the Yılanlı Burnu quarry where it is suggested that divalent cations (e.g., Mg²⁺) substitution into the octahedral sheet is related to dolomitic host-rocks.

5.2. Chemistry, origin and illitization age of K-bentonites

Illites and I-Sm show differences based on their chemistry where they can be distinguished based on their Si and interlayer cation contents. Illites have lower tetrahedral Al for Si substitution and higher

octahedral substitutions (Fe and Mg for Al) than those of I-S. The interlayer Ca is slightly higher in I-Sm. The octahedral Mg is highest in the Yılanlı Burnu quarry, indicating Mg diffusion from dolomitic host rocks. The origin of potassium is still not known for the studied K-bentonites, with possible sources being volcanogenic minerals like biotite, feldspars that were coexisting in the original ash or sediments in seawater. The lack of Ta and Nb negative REE anomaly are characteristic for volcanics with a mantle origin. Additionally, Zr/TiO₂ versus Nb/Y compositions of illites and I-Sm show similar data for bulk K-bentonite compositions indicating that the original ashes had alkali basaltic and trachytic compositions, respectively (Göncüoğlu et al., 2016).

The oxygen and hydrogen isotopic compositions of the authigenic crystals are dependent on the chemistry of the interacting fluids and on the crystallization temperature. In confined systems, as is the case for the studied bentonitic material, the mineral δ¹⁸O becomes more depleted during crystal growth with increasing temperature and/or the water/rock ratio (e.g., Savin and Lee, 1988; Sheppard and Gilg, 1996). The δ¹⁸O values of the illite and I-Sm show narrow ranges between 17.75 to 21.91‰ (V-SMOW), whereas δD values range widely from -10.1 to -69.9‰ (V-SMOW). Narrow ranges of δ¹⁸O values may imply short-term or sudden crystallization. The small differences reflect varied temperature conditions for two areas (e.g., Clauer et al., 2013). If crystallization temperatures of illites and I-Sm were assumed as ~120 to 140 °C for illite, and ~80 °C for I-Sm, then the illite forming fluids had δ¹⁸O values of ~9 and ~6‰ for illite and I-Sm, respectively. Wide ranges for δD

values reported for bentonite illite-type particles (e.g., Clauer et al., 2013, 2014), suggest that meteoric waters at the time of deposition may have been influenced by additional geographic conditions (i.e., latitude, altitude, elevation and evaporation).

K-Ar data of illitized bentonites from different size-fractions in the Bartın area showed that the coarser particles are older than the finer ones. This implies either (1) the coarser grains were of detrital origin, therefore they indicate the age of the source of parent rocks or (2) concomitant nucleation-crystal growth, thus the internal cores of the coarser particles (with $2M_1$ polytype) are the oldest fraction (e.g., Moe et al., 1996). The large age range (80–160 Ma) between initial sedimentation and illitization of tephras are in favor of their detrital origin. For K/Ar age determination of illites, fine-grained fractions ($<0.5 \mu\text{m}$), are represented mainly by diagenetic $1M_d$ polytypes. The illitization age (281–283 Ma; early Permian) for illites of K-bentonites from the Gavurpinarı and Yılanlı Burnu quarries in Bartın area coincides with a stratigraphic gap (or hiatus) or regional unconformity corresponding to a Variscan event (e.g. Göncüoğlu et al., 2011). For Zonguldak area, the illitization age (174–190 Ma; Early Jurassic) of R3 I-Sm is indicative for a younger geologic event that is coeval with the Cimmerian event in NW Anatolia (e.g., Okay et al., 2006, 2014).

6. Conclusions

In the NW area of Anatolia, Turkey four locations (Gavurpinarı and Yılanlı Burnu quarries near Bartın city, Çimşir Çukurları (Şapça) quarry and Güdüllü-Gökgöl highway tunnel section at Zonguldak city) with K-bentonite (tephra) layers were recently discovered within the Late Devonian-Early Carboniferous platform carbonates. The K-bentonites consist mainly of illite in the Bartın area and R1 and R3 I-Sm in the Zonguldak area. They have platy and sponge-like shapes, respectively. Crystal-chemical data of illites indicate high-grade diagenesis (120° to 140 °C), whereas low-grade diagenesis for I-Sm (~80 °C). The relative crystal chemistry of these clays, according to d_{060} values, show illite and I-Sm have dioctahedral composition, but illites from dolomitic limestone-hosted bentonites have relatively larger d_{060} values because of Mg diffusion during crystallization. Major and trace element compositions of illites and I-Sm show illites contain higher SiO₂ and CaO and lower FeO and MgO than I-Sm. Chondrite-normalized trace and REE patterns exhibit similar trends for illite and I-Sm, but show relatively higher values for I-S. The $\delta^{18}\text{O}$ and δD % (V-SMOW) compositions, illites have a narrower range, than the I-Sm. Oxygen isotope values indicate a short-term or sudden crystallization event that occurred under different varied temperature conditions for both areas, where illites were formed under somewhat higher temperatures (~60 °C) than I-Sm. Illitization ages of K-bentonites suggest an Early Permian (Variscan?) event in Bartın and an Early Jurassic (Cimmerian?) event in Zonguldak area, which corresponds to differences in the paleotectonic setting and evolutionary paths for both areas.

Acknowledgements

This study was supported by TÜBİTAK (Scientific Research Project grant no: 110Y272). The authors thank to Dr. Jesse Marion Wampler (Georgia State University, Atlanta, USA) for K-Ar dating, to Prof. Dr. Doug Crowe and Dr. Julia Cox (University of Georgia, Athens, USA) for O-H isotope geochemistry and METU Central Laboratory for XRD and SEM analytical support. The authors also thank to Prof. Dr. Warren D. Huff (University of Cincinnati, USA) for valuable contributions to study during field excursion and revision processes.

References

- Akbaş, B., Altun, I.E., Aksay, A., 2002. 1/100.000 Ölçekli Türkiye Jeoloji Haritaları. Zonguldak-E28 Pftası. MTA Jeoloji Etütleri Dairesi, Ankara, Turkey (in Turkish).
- Alişan, C., Derman, A.S., 1995. The first palynological age, sedimentological and stratigraphic data for the Çakraz Group (Triassic), western Black Sea. In: Erler, et al. (Eds.), Geology of the Black Sea Region, Proceedings of the Int. Symposium on the Geology of Black Sea Region. General Directorate of Mineral. Res. Explor, Ankara, pp. 93–98.
- Altaner, S.P., Ylagan, R.F., 1997. Comparison of models of mixed-layer illite/smectite and reaction mechanism of smectite illitization. *Clay Clay Miner.* 45, 517–533.
- Aydin, M., Serdar, H.S., Şahintürk, O., Yazman, M., Çokuğraş, R., Demir, O., Özçelik, Y., 1987. *Geology of the Çamdağ (Sakarya)-Sunnicedağ (Bolu) Region.* Bull. Geol. Soc. Turk. 30 (1), 1–4 (in Turkish).
- Bailey, S.W., 1988. X-ray diffraction identification of the polytypes of mica, serpentine, and chlorite. *Clay Clay Miner.* 36, 193–213.
- Bethke, C.M., Vergo, N., Altaner, S.P., 1986. Pathways of smectite illitization. *Clay Clay Miner.* 34, 125–135.
- Bozkaya, Ö., Yalçın, H., Göncüoğlu, M.C., 2012. Mineralogic evidences of a mid Paleozoic tectonothermal event in the Zonguldak terrane, NW Turkey: implications for the dynamics of some Gondwana-derived terranes during the closure of the Rheic Ocean. *Can. J. Earth Sci.* 49, 559–575.
- Christidis, G.E., 1998. Comparative study of the mobility of major and trace elements during alteration of an andesite and a rhyolite to bentonite in Island of Milos and Kimolos, Aegean, Greece. *Clay Clay Miner.* 46, 379–399.
- Clauer, N., 2006. Toward an isotopic modeling of the illitization process based on data of illite-type fundamental particles from mixed layered illite-smectite. *Clay Clay Miner.* 54 (199–130).
- Clauer, N., Środoń, J., Francú, J., Šucha, V., 1997. K-Ar dating of illite fundamental particles separated from illite/smectite. *Clay Miner.* 32, 181–196.
- Clauer, N., Fallick, A.E., Eberl, D.D., Honty, M., Huff, W.D., Aubert, A., 2013. K-Ar dating and $\delta^{18}\text{O}$ -δD characterization of nanometric illite from Ordovician K-bentonites of the Appalachians: illitization and the Acadian-Alleghenian tectonic activity. *Am. Mineral.* 98, 2144–2154.
- Clauer, N., Honty, M., Fallick, A.E., Šucha, V., Aubert, A., 2014. Regional illitization in bentonite beds from the East Slovak Basin based on isotopic characteristics (K-Ar, $\delta^{18}\text{O}$ and δD) of illite-type nanoparticles. *Clay Miner.* 49, 247–275.
- Condie, K.C., 1993. Chemical composition and evolution of the upper continental crust: contrasting results from surface samples and shales. *Chem. Geol.* 104, 1–37.
- Craig, H., 1961. Isotopic variations in meteoric waters. *Science* 133, 1702–1703.
- De Man, E., Van Simaeys, S., Vandenberghe, N., Harris, W.B., Wampler, J.M., 2010. On the nature and chronostratigraphic position of the Rupelian and Chattian stratotypes in the southern North Sea Basin. *Episodes* 33, 3–14.
- Dean, W.T., Martin, F., Monod, O., Demir, O., Richards, R.B., Bultynck, P., Bozdoğan, N., 1997. Lower Paleozoic stratigraphy, Karadere-Zirze area, Central Pontides, N Turkey. In: Göncüoğlu, M.C., Derman, A.S. (Eds.), Early Paleozoic Evolution in NW Gondwana. Turkish Assoc Petrol Geol Spec Publ vol. 3, pp. 32–38.
- Derman, A.S., 1997. Sedimentary characteristics of Early Paleozoic rocks in the western Black Sea region, Turkey. In: Göncüoğlu, M.C., Derman, A.S. (Eds.), Early Paleozoic Evolution in NW Gondwana. Turkish Assoc Petrol Geol Spec Publ vol. 3, pp. 24–31.
- Dil, N., 1976. Assemblages caractéristiques de foraminifères du Devonien supérieur et du Dinantien de Turquie (Bassin Carbonifère de Zonguldak). *Ann. Soc. Geol. Belg.* 99, 373–400.
- Dong, H., Hall, C.M., Peacor, D.R., Halliday, A.N., 1995. Mechanisms of argon retention in clays revealed by laser ^{40}Ar - ^{39}Ar dating. *Science* 267, 355–359.
- Eberl, D.D., Velde, B., 1989. Beyond the Kübler index. *Clay Miner.* 24, 571–577.
- Elliot, W.C., Aronson, J.L., 1987. Alleghenian episode of K-bentonite illitization in the southern Appalachian Basin. *Geology* 8, 735–730.
- Ferreiro Mählmann, R., Bozkaya, Ö., Potel, S., Le Bayon, R., Šegvić, B., Nieto, F., 2012. The pioneer work of Bernard Kübler and Martin Frey in very low-grade metamorphic terranes: paleo-geothermal potential of variation in Kübler-Index/organic matter reflectance correlations. A review. *Swiss J. Geosci.* 105, 121–152.
- Fortey, N.J., Merriman, R.J., Huff, W.D., 1996. Silurian and Late-Ordovician K-bentonites as a record of late Caledonian volcanism in the British Isles. *T RSE Earth* 86, 167–180.
- Frey, M., 1987. Very low-grade metamorphism of clastic sedimentary rocks. In: Frey, M. (Ed.), Low Temperature Metamorphism. Blackie, Glasgow, pp. 9–58.
- Gat, J.R., Shemesh, A., Tziperman, E., Hecht, A., Georgopoulos, D., Basturk, O., 1996. The stable isotope composition of waters of the eastern Mediterranean Sea. *J. Geophys. Res.* 101, 6441–6451.
- Gedik, I., Pehlivan, S., Duru, M., Timur, E., 2005. 1:50.000 Scaled Geological Maps and Explanations: Sheets Bursa G22a and İstanbul F22d. General Directorate of Mineral Research Exploration (MTA), Ankara.
- Göncüoğlu, M.C., Kozlu, H., 2000. Early Paleozoic evolution of the NW Gondwana land: data from southern Turkey and surrounding regions. *Gondwana Res.* 3, 315–324.
- Göncüoğlu, M.C., Kozlu, H.W., 1998. Facial development and thermal alteration of Silurian rocks in Turkey. In: Gutierrez-Marco, J.C., Rabano, I. (Eds.), Proceedings of the 1998 Silurian Field-Meeting. Temas Geológico-Mineros ITGE 23, pp. 87–90.
- Göncüoğlu, M.C., Kozlu, H.W., 1999. Remarks on the pre-Variscan development in Turkey. In: Linnemann, U., Heuse, T., Fatkı, O., Kraft, P., Brocke, R., Erdtmann, B.T. (Eds.), Prevariscan Terrane Analyses of Gondwanean Europa. Schriften des Staatlichen Museums, Mineralogie, Geologie, Dresden 9, pp. 137–138.
- Göncüoğlu, M.C., Dirik, K., Kozlu, H., 1997. General characteristics of pre-alpine and alpine terranes in Turkey: explanatory notes to the terrane map of Turkey. *Ann. Géol. Pays Hellen.* 37, 515–536.
- Göncüoğlu, M.C., Okuyucu, C., Dimitrova, T., 2011. Late Permian (Tatarian) deposits in NW Anatolia: palaeogeographical implications. *Geocomarina* 17, 79–82.
- Göncüoğlu, M.C., Sachanski, V., Gutiérrez-Marco, J.C., Okuyucu, C., 2014. Ordovician grapholithes from the basal part of the Palaeozoic transgressive sequence in the Karadere area, Zonguldak Terrane, NW Turkey. *Estonian J. Earth Sci.* 63, 227–232.

- Göncüoğlu, M.C., Günal-Türkmenoğlu, A., Bozkaya, Ö., Ünlüce-Yücel, Ö., Okuyucu, C., Yılmaz, İ.Ö., 2016. Geological features and geochemical characteristic of Late Devonian-Early Carboniferous K-Bentonites from Northwestern Turkey. *Clay Miner.* (accepted).
- Grathoff, G.H., Moore, D.M., 1996. Illite polypole quantification using Wildfire® calculated X-ray diffraction patterns. *Clay Clay Miner.* 44, 835–842.
- Gromet, L.P., Dymek, R.F., Haksin, L.A., Korotev, R.L., 1984. The North American shale composite: its compilation, major and trace element characteristics. *Geochim. Cosmochim. Acta* 48, 2469–2482.
- Guggenheim, S., Bain, D.C., Bergaya, F., Brigatti, M.F., Drits, V., Eberl, D.D., Formoso, M., Galan, E., Merriman, R.J., Peacor, D.R., et al., 2002. Report of the Association Internationale pour l'Etude des Argiles (AIPEA) Nomenclature Committee for 2001: order, disorder, and crystallinity in phyllosilicates and the use of the "crystallinity" index. *Clay Clay Miner.* 50, 406–409 (and *Clay Miner.* 37: 389–393).
- Guidotti, C.V., Mazzoli, C., Sassi, F.P., Blencoe, J.G., 1992. Compositional controls on the cell dimensions of 2M1 muscovite and paragonite. *Eur. J. Mineral.* 4, 283–297.
- Günlük-Türkmenoğlu, A., Bozkaya, Ö., Göncüoğlu, M.C., Ünlüce, Ö., Yılmaz, İ.Ö., Okuyucu, C., 2015. Clay mineralogy, chemistry, and diagenesis of Late Devonian K-bentonite occurrences in northwestern Turkey. *Turk. J. Earth Sci.* 24, 209–229.
- Histon, K., Klein, P., Schonlaub, H.P., Huff, W.D., 2007. Lower Palaeozoic K-bentonites from the Carnic Alps, Austria. *Aust. J. Earth Sci.* 100, 26–42.
- Hoffman, J., Hower, J., 1979. In: Scholle, P.A., Schlager, R. (Eds.), *Clay Mineral Assemblages as Low Grade Metamorphic Geothermometers: Application to the Thrust-Faulted Disturbed Belt of Montana, U.S.A. Aspects of Diagenesis* 26. S.E.P.M. Spec. Publ. pp. 55–80.
- Honty, M., Uhlik, P., Šucha, V., Caplivčová, M., Francú, J., Clauer, N., Biroň, A., 2004. Smectite to illite alteration in salt-bearing bentonites (the East Slovak Basin). *Clay Clay Miner.* 52, 533–551.
- Huff, W.D., Türkmenoğlu, A.G., 1981. Chemical characteristics and origin of Ordovician K-bentonites along the Cincinnati Arch. *Clay Clay Miner.* 29, 113–123.
- Inoue, A., Watanabe, T., Kohyama, A., Brusewitz, A.M., 1990. Characterization of illitization of smectite in bentonite beds at Kinnekulle, Sweden. *Clay Clay Miner.* 38, 241–249.
- Jagodzinski, H., 1949. Eindimensionale Fehlordnung in Kristallen und ihr Einfluss auf die Riintgeninterferenzen. I. Berechnung des Fehlordnungsgrades aus der Röntgenintensitäten. *Acta Crystallogr.* 2, 201–207.
- Keller, W.D., Reynolds Jr., R.C., Inoue, A., 1986. Morphology of clay minerals in the smectite-to-illite conversion series by scanning electron microscopy. *Clay Clay Miner.* 34, 187–197.
- Kerey, I.E., 1984. Facies and tectonic setting of the upper Carboniferous rocks of NW Turkey. In: Robertson, A.H.F., Dixon, J. (Eds.), *The Geological Evolution of the Eastern Mediterranean*. Geol Soc Spec Publ, Blackwell Scientific Publ., Oxford, pp. 123–128.
- Kisch, H.J., 1991. Illite crystallinity: recommendations on sample preparation X-ray diffraction settings and inter-laboratory samples. *J. Metamorph. Geol.* 9, 665–670.
- Krumm, S., 1996. WINFIT 1.2: version of November 1996 (The Erlangen Geological and Mineralogical Software Collection) of WINFIT 1.0: a public domain program for interactive profile analysis under WINDOWS. XIII Conference on Clay Mineralogy and Petrology.
- Kübler, B., 1968. Evaluation quantitative du métamorphisme par la cristallinité de l'illite. *Bull. Centre Rech. Pau-SNPA* 2, 385–397.
- Lindgreen, H., Hansen, P.L., 1991. Ordering of illite-smectite in Upper Jurassic claystones from the North Sea. *Clay Miner.* 26, 105–125.
- Merriman, R.J., Frey, M., 1999. Patterns of very low-grade metamorphism in metapelitic rocks. In: Frey, M., Robinson, D. (Eds.), *Low Grade Metamorphism*. Blackwell, Oxford, pp. 61–107.
- Merriman, R.J., Peacor, D.R., 1999. Very low-grade metapelites: mineralogy, microfabrics and measuring reaction progress. In: Frey, I.M., Robinson, D. (Eds.), *Low Grade Metamorphism*. Blackwell, Oxford, pp. 10–60.
- Merriman, R.J., Roberts, B., 1990. Metabentonites in the Moffat Shale Group, Southern Uplands of Scotland: geochemical evidence of ensialic marginal basin volcanism. *Geol. Mag.* 127, 259–271.
- Moe, J.A., Ryan, P.C., Elliott, W.C., Reynolds Jr., R.C., 1996. Petrology, chemistry, and clay mineralogy of a K-bentonite in the Proterozoic Belt Supergroup of Western Montana. *J. Sediment. Res.* 66, 95–99.
- Moore, D.M., Reynolds Jr., R.C., 1997. *X-Ray Diffraction and the Identification and Analysis of Clay Minerals*. 2nd edition. Oxford University Press, Oxford, New York (378 pp).
- Nadeau, P.H., Wilson, M.J., McHardy, W.J., Tait, J.M., 1985. The conversion of smectite to illite during diagenesis: evidence from some illitic clays from bentonites and sandstones. *Mineral. Mag.* 49, 393–400.
- Nzegge, O.M., Satir, M.A., Siebel, W.A., Taubald, H.A., 2006. Geochemical and isotopic constraints on the genesis of the Late Palaeozoic Deliktaş and Sivrikaya granites from the Kastamonu Granitoid Belt (Central Pontides, Turkey). *Neues Jb. Mineral. Abh.* 183, 27–40.
- Okay, A.I., Satir, M., Siebel, W., 2006. Pre-Alpine Paleozoic and Mesozoic orogenic events in the Eastern Mediterranean region. In: Gee, D.G., Stephenson, R.A. (Eds.), *European Lithosphere Dynamics* 32. Geol Soc London, Memoirs, pp. 389–405.
- Okay, N., Zack, T., Okay, A.I., 2010. A missing provenance: sandstone petrography and detrital zircon-rutile geochronology of the Carboniferous flysch of the Istanbul zone. *Tectonic Crossroads: Evolving Orogenes of Eurasia-Africa-Arabia*. Geological Society of America, Ankara, p. 67 Abstract No 35–2.
- Okay, A.I., Altiner, D., Kılıç, A.M., 2014. Triassic limestone, turbidites and serpentinite—the Cimmeride orogeny in the Central Pontides. *Geol. Mag.* 152, 460–479.
- Pevear, D., 1999. Illite and hydrocarbon exploration. *Proceedings of the National Academy of Sciences of the United States of America*. vol. 96, pp. 3440–3446 ([0027-8424] iss: 7 pg).
- Reynolds, R.C., 1980. Interstratified clay minerals. In: Brindley, G.W., Brown, G. (Eds.), *Crystal Structures of Clay Minerals and their X-ray Identification*. Mineralogical Society, London, pp. 249–303.
- Reynolds, R.C., 1985. NEWMOD a Computer Program for the Calculation of one-Dimensional Diffraction Patterns of Mixed-Layer Clays, R.C. Reynolds, 9 Brook Rd., Hanover, New Hampshire 03755, USA.
- Sachanski, V., Göncüoğlu, M.C., Gedik, I., 2010. Late Telychian (early Silurian) graptolitic shales and the maximum Silurian highstand in the NW Anatolian Palaeozoic terranes. *Palaeogeogr. Palaeoclimatol.* 291, 419–428.
- Savin, S.M., Epstein, S., 1970. The oxygen and hydrogen isotope geochemistry of clay minerals. *Geochim. Cosmochim. Acta* 34, 25–42.
- Savin, S.M., Lee, M., 1988. Isotopic studies of phyllosilicates. In: Bailey, S.W. (Ed.), *Hydrous Phyllosilicates Reviews in Mineralogy* vol. 19. Mineralogical Society of America, Washington, DC, pp. 189–223.
- Schroeder, P.A., 1992. A multiple reaction mechanism (MRM) model for illitization during burial diagenesis. In: Nagasawa, K. (Ed.), *Clay Minerals and their Natural Resources*. 29th International Geological Congress Workshop WB-1, Kyoto, Japan 79–88.
- Sheppard, S.M.F., Gilg, H.A., 1996. Stable isotope geochemistry of clay minerals. *Clay Miner.* 31, 1–24.
- Sheppard, S.M.F., Nielsen, R.L., Taylor Jr., H.P., 1969. Oxygen and hydrogen isotope ratios of clay minerals from porphyry copper deposits. *Econ. Geol.* 64, 755–777.
- Šrodoň, J., 1984. X-ray powder diffraction identification of illitic materials. *Clay Miner.* 32, 337–349.
- Šrodoň, J., Clauer, N., Eberl, D.D., 2002. Interpretation of K-Ar dates of illitic clays from sedimentary rocks aided by modeling. *Am. Mineral.* 87, 1528–1535.
- Šrodoň, J., Kotarba, M., Biroň, A., Such, P., Clauer, N., Wojtowicz, A., 2006. Diagenetic history of the Podhale-Orava Basin and the underlying Tatra sedimentary structural units (Western Carpathians): evidence from XRD and K-Ar of illite-smectite. *Clay Miner.* 41, 751–774.
- Sun, S.S., McDonough, W.F., 1989. Chemical and isotopic systematics of oceanic basalts: implications for mantle composition and process. In: Saunders, A.D., Norry, M.J. (Eds.), *Magmatism in Ocean Basins*. Geol Soc London Spec Publ vol. 42, pp. 313–345.
- Türkmenoğlu, A.G., 2001. A Paleozoic K-bentonite occurrence in Turkey, Mid-European Clay Conference'01, MECC, September 9–14, Stara Leusa, Slovakia. Book of Abstracts, p. 108.
- Türkmenoğlu, A.G., Göncüoğlu, M.C., Bayraktaroglu, Ş., 2009. Early Carboniferous K-bentonite formation around Bartın: geological implications. 2nd International Symposium on the Geology of the Black Sea Region, p. 209.
- Valley, J.W., Kitchen, N., Kohn, M.J., Niendorf, C.R., Spicuzza, M.J., 1995. UWG-2, a garnet standard for oxygen isotope ratio: strategies for high precision and accuracy with laser heating. *Geochim. Cosmochim. Acta* 59, 5223–5231.
- Vennemann, T.W., O'Neil, J.R., 1993. A simple and inexpensive method of hydrogen isotope and water analyses of minerals and rocks based on zinc reagent. *Chem. Geol.* 103, 227–234.
- Warr, L.N., Ferreiro-Mählmann, R., 2015. Recommendations for Kübler Index standardization. *Clay Miner.* 50, 283–286.
- Warr, L.N., Rice, A.H.N., 1994. Interlaboratory standardisation and calibration of clay mineral crystallinity and crystallite size data. *J. Metamorph. Geol.* 12, 141–152.
- Weaver, C.E., 1953. Mineralogy and petrology of some Ordovician K-bentonites and related limestones. *Geol. Soc. Am. Bull.* 64, 921–944.
- Weaver, C.E., Pollard, L.D., 1973. *The Chemistry of Clay Minerals (Developments in Sedimentology, 15)*. Elsevier, Amsterdam & New York (272 pp).
- Yalçın, M.N., Yılmaz, I., 2010. Devonian in Turkey – a review. *Geol. Carpath.* 61, 235–253.
- Yanev, S., Göncüoğlu, M.C., Gedik, I., Lakova, I., Boncheva, I., Sachanski, V., Okuyucu, C., Ozgul, N., Timur, E., Malakov, Y., et al., 2006. Stratigraphy, correlations and palaeogeography of Palaeozoic terranes of Bulgaria and NW Turkey: a review of recent data. In: Robertson, A.H.F., Mountrakis, D. (Eds.), *Tectonic Development of the Eastern Mediterranean Region* 260. Geol Soc London, Spec Publ, pp. 51–67.
- Yeh, H.-W., 1980. D/H ratios and late stage dehydration of shales during burial. *Geochim. Cosmochim. Acta* 44, 341–352.